VOL. 35, Nº 1

JUNIO 2013

ISSN 0717-2915

Revista
Journal

SELPER

Cayena
Imagen de satélite LandSat 8 OLI

REVISTA JOURNAL

SOCIEDAD LATINOAMERICANA DE PERCEPCION REMOTA Y SISTEMAS DE INFORMACION ESPACIAL • SOCIEDADE LATINO-AMERICANA EM SENSORIAMENTO REMOTO E SISTEMAS DE INFORMAÇAO ESPACIAL • LATINAMERICAN SOCIETY ON REMOTE SENSING AND SPACE INFORMATION SYSTEM

SELPER

VOL. 35 Nº 1 Junio 2013 ISSN 0717-2915

FOTO PORTADA

Cayena

Imagen de satélite Landsat 8 OLI, resolución espacial 30 metros, en composición 4,3,2 - RGB, de la ciudad de Cayena tomada el 26 de julio de 2014. Los sectores que se destacan son: Matoury, Remire Montjoly y Roura.

DIRECTORIO SELPER, SEDE Francia 2012 - 2014

Institut de recherche pour le développement Le Sextant

44, bd de Dunkerque, CS 90009 - 13572 Marseille cedex 02

Tél. 33 (0)4 91 99 92 00 - Fax 33 (0)4 91 99 92 22

selper.internacional@gmail.com

PRESIDENTE

Laurent Durieux

Francia

VICE–PRESIDENTE

Marie José Lefevre Fonallosa

Francia

VICE-PRESIDENTE

Silvia Casas

México

VICE-PRESIDENTE

Luz Angela Rocha

Colombia

RESPONSABLE DE DIVULGACIÓN ELECTRÓNICA

Fabián Lozano García

Mexico

COMITÉ DE RELACIONES INTERNACIONALES

Luz Angela Salamanca (Colombia)
Presidente interina
Laurent Durieux – Francia
Pedro Luis García Pérez - Cuba
Pedro Martínez Fernández - Cuba
Olga Piedad Rudas - Colombia
Anyul del Pilar Mora - Colombia
Luis Geraldo Ferreira - Brasil
Washintong Franca Rocha - Brasil
Victor Barrena - Perú

COMITÉ EDITORIAL

María Cristina Serafini (Argentina)
Presidente
Miriam Esther Antes – Argentina
Fabián Lozano – México
Leila María Fonseca – Brasil
Jorge Martín Chiroles - Cuba
Francisca Celia González - Argentina
Freddy Flores – Venezuela

COMITÉ DE EDUCACIÓN

Maria Antonia García Cisnero (Cuba)
Presidente
Luz Angela Rocha Salamanca - Colombia
Laura Delgado - Venezuela
Ethel Rubín de Celís Llanos - Perú
Josselisa Ma. Chávez - Brasil

COMITÉ DE PROYECTOS INTERNACIONALES

Paulo Roberto Martini (Brasil)
Presidente
Christopher Charron – Francia
Alfredo Cuello – Argentina
Miembro del ISPRS

CAPÍTULOS CONSTITUIDOS

ARGENTINA
Miriam Esther Antes
Universidad Nacional de Luján (PRODITEL)
Fuerza Aérea Argentina (CSR)
Cruce Rutas 5 y Ex. 7 (6700)
Luján, Buenos Aires, Argentina
Tel: 54 - 2323- 420380 - int. 248
Fax: 54 - 2323- 425795
E-mail: selperargentina@gmail.com

BOLIVIA
José Luis Liseca
Carrera de Topografía y Geodesia
Facultad Técnica
Universidad Mayor de San Andrés
Av. Arce 2299 1º Piso
La Paz, Bolivia
Tel.: 591-2-2441401
E-mail: jlisec@hotmail.com

BRASIL
Laércio Massuru Namikawa
INPE
Av. Dos Astronautas 1758, Sao José dos Campos
San Pablo, Brasil
Tel: 55 - 12-39456000
E-mail: laercio@dpi.inpe.br

CHILE
Héctor Gutiérrez Méndez
Centro Nacional de Información Aeroespacial
Antonio Varas 175
Oficina 310. Providencia
Tel: 562 -2362714
E-mail: hector.gutierrez@cenia.cl

COLOMBIA
Luz Angela Rocha Salamanca
Carrera 30 No. 48-51 Edificio IGAC-CIAF Of. 212
Bogotá D.C., Colombia
Tel: 57-1-369-4096
Fax: 57-1-369-4096
E-mail: lrochas@selper.org

CUBA
Pedro Luis García Pérez
Sede UNAICC, Humboldt No. 104,
Esquina a Infanta, Vedado, La Habana, Cuba
Telf.: (5 37) 8363447
E-mail: lgarcia@ch.unaicc.cu

ECUADOR
Cor. Ricardo Urbina
CLIRSEN
Edif. Instituto Geográfico Militar, Piso 4
Seniergues s/n y Paz y Miño
Apartado Postal 17-08-8216

GUATEMALA
Carlos Alberto Duarte
Ingeniería Virtual
Ruta 4, 6-49 Zona 4, Oficina 14
Ciudad de Guatemala (01004), Guatemala
Tel: 502 - 334-1039/4038
Fax: 502 - 331-9390
E-mail: chduarte@hotmail.com

GUYANA FRANCESA
Laurent Polidoril
Directeur de Recherche IRD / US ESPACE 140
Institut de Recherche pour le Développement (ex-ORSTOM)
Route de Montabo - BP 165 - 97323 Cayenne cedex
Tel. (+594) 594 29 92 81
Fax (+594) 594 31 98 55
E-mail:polidori@cayenne.ird.fr

MÉXICO
Jean Francois Mass
UNAM Campus Morelia
Morelia, Michoacan, México
E-mail: jfmas@ciga.unam.mx

FRANCIA
Marie José Lefevre Fonollosa
CNES
18 avenue Edouard Belin, 31401 Toulouse Cedex 9
Tél : 3305 61 27 4283
Fax : 3305 61274842
E-mail: marie-jose.lefevre @cnes.fr

URUGUAY
Antonio Alarcón
Servicio de Sensores Remotos Aeroespaciales Fuerza Aérea Uruguaya
Ruta 101 s/n Km. 19500
Carrasco, Canelones, Uruguay
Tel.: 598 -2 601 4083
Fax: 598 -2 601 4090
E-mail: aalarconv@hiotmail.com

VENEZUELA
Ramiro Salcedo
Centro de Procesamiento Digital del Instituto de Ingenieria en Caracas
Apdo. Postal 40200 / Caracas, Venezuela
Tel/fax: 58 - 212 - 903 -4682
E-mail: ramiros@fii.org

PERÚ
Victor Barrena Arroyo
Universidad Nacional Agraria La Molina
Av. La Universidad s/n
La Molina, Lima, Perú
Tel / Fax: 51-1-349-5647 anexo 232/349-2041

CAPÍTULOS EN FORMACIÓN

PARAGUAY
Sergio M. Burgos Sosa
IPPA
Dr. César Sánchez 431
San Lorenzo, Paraguay
Tel/Fax: 595- 21-574909
Email: smburgos@highway.com.py

CAPÍTULOS ESPECIALES

ALEMANIA
Klaus Reiniger
DLR
D-8031 Oberpfaffenohfen
Alemania
Tel: 49- 8153- 281.189
Fax: 49- 8153- 281.443

CANADÁ
Fritz P. Dubois
25 Nidland
Crs Nepean Ontario Kh2-8n2
Ontario, Canadá
Tel: 613- 596-4164
Fax: 613- 723-9626

ESPAÑA
José L. Labrandero
Consejo Superior de Investigaciones Científicas (CSIC)
Pinar 25- Madrid 28006, España
Tel: 34- 411.10.98
Fax: 34- 562.55.67

HOLANDA
Carlos Valenzuela
ITC
350 Boulevard 1945, P.O.X. 6. 7500 AA
Enschede, Holanda
Tel.: 31 53 874-444
Fax: 31 53 874-400

ITALIA
Francesco Sarti
ESA/ESRIN
Via Galileo Galilei, s/n
I-00044 Frascati, Italia
Tel: 39 - 694180409
Fax: 39 - 694180602
E-mail: Francesco.Sarti@esa.int

Maurizio Fea
via Alessandro Poerio, 49
00152 Roma
tel/fax: +39065880581
móvil: +393281771383
E-mail: maufea@gmail.com

USA
Patricia M. Ravelo
SPOT
Estados Unidos
Tel: 1-800-ask-spot ext. 137
Fax: 703-648.1813
E-mail: ravelo@spot.com

Editado por: SELPER Internacional
Universidad Nacional de Luján
Rutas 5 y ex 7, (6700) Luján - Bs. As. ARGENTINA

PLAN EDITORIAL SELPER 2012 - 2014

PLAN EDITORIAL SELPER

A partir de las decisiones adoptadas en el marco del XIII Simposio Latinoamericano de Percepción Remota y Sistemas de Información Espacial, llevado a cabo en La Habana, Cuba, en setiembre de 2008, la edición de la Revista SELPER está disponible en la página de nuestra Sociedad: http://www.selper.info.

En esta oportunidad hacemos llegar la publicación del volumen 35 Número 1., donde se incluyen trabajos que han sido presentados en el XIV Simposio Latinoamericano de Percepción Remota y Sistemas de Información Espacial (SELPER), desarrollado en Cayena, Guyana Francesa, en noviembre de 2012.

NORMAS PARA LOS AUTORES

Los artículos recibidos serán enviados a tres (3) expertos en la temática para su revisión. Los trabajos aprobados serán publicados en estricto orden, de acuerdo a las fechas de llegada de las contribuciones.

Los idiomas oficiales SELPER son: Español, Portugués e Inglés.

Los trabajos deberán estructurarse contemplando las siguientes secciones:

a) Título del trabajo. Nombre de los autores y direcciones completas

b) Resumen (no más de 150 palabras) indicando al final las palabras claves. Deberá incluirse en Español o Portugués, además de Inglés

c) Introducción

d) Objetivos

e) Metodología empleada y materiales

f) Resultados obtenidos

g) Conclusiones

h) Bibliografía: sólo se incluirá la citada en el texto. Se indicarán los autores, por orden alfabético, año, título, revista o medio donde fue publicado, incluyendo volumen y páginas, cuando corresponda.

Los títulos y subtítulos de cada sección deberán estar claramente indicados (ya sea con numeración o tamaño de letras). Las tablas, fotos y figuras deberán ser suficientemente nítidas, llevar un título y estar numeradas en forma consecutiva.

Se deberá enviar una copia del trabajo en formato Word y una copia papel. La extensión total del trabajo no deberá superar las 12 páginas, (DIN-A4).

Los trabajos se enviarán a: editorial@selper.org

A land cover map from Ellesmere Island to Tierra del Fuego: the combination of two continental land cover mapping projects and comparison to global maps

René Roland Colditz
Ricardo Magdaleno Llamas Barba

National Commission for the Knowledge and Use of Biodiversity (CONABIO)
Avenida Liga Periférico-Insurgentes Sur 4903, Col. Parques del Pedregal, Del. Tlapan, 14010, México, D.F. rcolditz@conabio.gob.mx, ricardo.llamas@conabio.gob.mx

ABSTRACT

Land cover affects and is affected by climate change and therefore is a critical input to climate, biogeochemical, hydrological, and species distribution models. There are multiple global land cover datasets such as GLC2000, the MODIS land cover product, and GlobCover. Although all are useful for modeling at the global scale, the spatial resolution, thematic detail, and accuracy is often insufficient for regional studies. The North American Land Change Monitoring System (NALCMS) was founded in 2006 with the goal to provide annually updated land cover information for the North American continent, which is Canada, the United States, and Mexico. As a first effort a continental map of the land cover in 2005 based on 250m MODIS data was completed. The Latin American network to monitor and study natural resources (SERENA) was founded in 2008 with the aim to monitor, study, and distribute information associated with changes due to burnt biomass as well as land cover of Latin America and the Caribbean. The network is formed by 52 participants from 11 countries and 18 institutions distributed over the whole region. The recently completed 2008 land cover map is based on 500m MODIS data. This study combines both products and presents a land cover map from Ellesmere Island to Tierra del Fuego. Critical steps in map combination included legend harmonization, adequate selection of projection and resolution parameters, and adjustments for differences among the years. The new map was compared to an existing land cover product, the MODIS land cover map of the year 2005. For important classes in terms of their total area the spatially-explicit correspondence among the maps is moderate (approximately 70%). Other classes such as mixed forest and grassland indicate poor agreements due to their intrinsic heterogeneity. These dissimilarities may be attributed to the methods (supervised or hybrid) and data but also to remaining differences in legends and processing issues to enable map comparison.

Keywords: Land cover, Map comparison, MCD12Q1, NALCMS, SERENA, MODIS, America

INTRODUCTION

Land cover and land use maps are probably the most common derivatives of satellite images. Land cover maps are required by the modeling community for climate, biodiversity, and partly also hydrology and landscape analysis. Another field of people interested in land cover maps the global change community. Land cover is defined at the physical material at the Earth surface. Typical materials are grass, trees, barren ground, or water. In this sense it is different from land use that is the description of the human use of land. Most maps are in reality a mix of both and thus termed a land use and land cover map (Fisher et al. 2005). Prominent examples are the mapping of land use classes urban area and agricultural land while other classes describe typical land covers, e.g. grassland and water. Land cover maps can be derived from satellite images in a fairly automatic manner and general land uses as described above may be inferred with reasonable accuracy.

Maps can be derived from various spatial resolutions, map extents and thematic detail that is the number of classes. Usually there is proportional relationship with increasing spatial resolution, decreasing extent and more detailed thematic classes. This is directly liked to feasibility. At least until nowadays there is no global map at 30m resolution but there exist multiple maps between 300 and 1000m. On the other hand it makes little sense to map a small city at that coarse resolution. The thematic detail not exclusively refers to the number of classes but also to the detail that the classes characterize.

This paper will focus on the combination of two existing land cover – and in the strict sense used above – also land use maps for the American continent. The maps originate from two existing mapping projects in which the authors participate. The North American Land Change Monitoring System (NALCMS) is a tri-national initiative of Canada (Canada Centre for Remote Sensing / Natural Resources Canada – CCRS/NRCan), the United States of America (United States Geological Survey – USGS), and Mexico (National Institute for Statistics and Geography – INEGI, National Commission for the Knowledge and Use of Biodiversity – CONABIO, National Forestry Commission – CONAFOR). The work is supported by the Commission for Environmental Cooperation (CEC) that is a tri-national institution to support environmental studies for the continent. The aims of NALCMS are to develop a land cover monitoring system at the continental scale using satellite images. It mainly employs images of the Moderate Resolution Imaging Spectroradiometer (MODIS) sensor. Using algorithms developed at CCRS seven reflective bands important for land cover monitoring are filtered for clouds and errors, downscaled to 250m spatial resolution and aggregated to monthly composites (Latifovic et al, 2012). In 2010 a baseline map, the land cover of North America for the year 2005, was completed and made publically available as wall map and in digital format (CEC 2010). The map has 19 thematic classes that characterize different types of forest, shrubland, grassland, lichen and moss, wetland, cropland, barren land, urban area, water, and snow / ice. The overall accuracy of the continental map is 68% for not considering ambiguity in the labeling of reference data and 82% if an alternative label is considered as correctly classified (Latifovic et al, 2012). Current activities of this on-going mapping initiative are the detection of change area and the characterization of changes for map updating. The long-term goal is an annually-generated map product. However, also continuous products and higher spatial resolution maps are anticipated.

Within the NALCMS initiative there are common guidelines for product development such as the baseline dataset, the legend that follows the Land Cover Classification System (LCCS, di Gregorio 2005) standards, and partly the algorithm. However, each country develops its own dataset also considering the national needs by not losing the overarching international requirements. Specific national requirements can be a thematically more detailed map that is aggregated for the continental map or a particular mapping approach to represent the diversity of the land cover. The latter was necessary for land cover mapping in Mexico where in many cases exists more than one label for a pixel of 6.25ha (Colditz et al. 2012). Using a multitude of discrete classifiers, C5.0 decision trees (Quinlan et al. 1993) the proportion of each land cover class was estimated. These class memberships represent commonly known ecological transition zones (ecotones) due to elevation changes or scarcity of water and heterogeneous areas with many mixed pixels, because the patchiness of the actual land cover is well beyond the resolution of 250m pixels (Colditz et al. 2011, Colditz et al 2012). Membership maps can be transformed to discrete land cover maps by assigning to each pixel the class with the highest proportion.

The same relatively new but computationally expensive approach was employed in the project "Latin American network to monitor and study natural resources" (SERENA). Founded in 2008 and embedded in the regional Global Observation of Forest and Land Cover Dynamics (GOFC-GOLD) program RedLaTIF, the network brings together 52 researchers from 10 countries distributed over the whole Latin American continent. The aim of this initiative is to monitor, study, and distribute information associated with changes due to burnt biomass and land cover from Mexico to Tierra del Fuego. The analysis is based on a set of monthly composites of MODIS images with a spatial resolution of 500m filtered for clouds and processing issues. The land cover sub-group recently finished the land cover map of Latin America for 2008 (Blanco et al. 2012). The wall map was released in spring 2012, and the digital release is anticipated for the end of 2012. The overall map accuracy was 84% on the continental scale and major confusions in the error matrix are related to ecological gradients and less to climate zones.

Both, NALCMS and SERENA maps are comparable because a similar legend was used in both projects. The map of 19 classes in the continental NALCMS was amplified to 22 classes in SERENA. The main difference is explicitly mapping sub-tropical classes in SERENA. In NALCMS there are combined tropical and sub-tropical classes, because their distinction was not imperative due to the small area proportion of their extent. In SERENA, however the majority of the mapping area is located within the tropical and sub-tropical climate zones.

The following chapter will describe how the maps were combined and which adjustments were necessary to link classes thematically. The results chapter will present the final map for the American continent and will compare this map quantitatively to an existing global land cover map. The final chapter outlines the conclusions.

2. METHODS FOR MAP COMBINATION AND ANALYSIS

The NALCMS as well as the SERENA maps were generated in the Lambert Azimuthal Equal Area (LAEA) projection but with two different projection origins. Also, the NALCMS map has a spatial resolution of 250m in contrast to SERENA with 500m. For the generation of the America map both maps were reprojected to a new projection center (10°S, 90°W) and a spatial resolution of 500m.

A second step concerned legend merge of the 19 classes NALCMS and 22 classes in SERENA.

The main difference between legends of both maps concerns the sub-tropical classes that were discerned in SERENA but not in NALCMS. However, the issue can be solved, because tropical classes in the NALCMS map extent only exist in Mexico, and Mexico was also covered by SERENA. Therefore the new America map employed data of SERENA for Mexico.

NALCMS data were only used for Canada and the United States where all tropical and sub-tropical classes were labeled “sub-tropical”. Other classes of lichens and mosses in NALCMS only exist in northern Canada and Alaska and not at all in South America.

Quantitative comparison of the America map to the MCD12Q1 map to another existing map was based on the comparison matrix. First, both maps were transformed to a common generalized legend of basic land cover classes. Cells of the diagonal of the matrix indicate the agreement (A) between both maps (Equation 1). In contrast, disagreement (D) can be calculated for both maps (X, Y) and is the sum of the column or row totals (+k, k+) minus the diagonal cell (Equations 2 and 3). An additional division by 2 is necessary for not double counting commission and omission among different classes.

$$A(X,Y)_k = n_{kk} \qquad (1)$$

$$D(X)_k = \frac{n + k - n_{kk}}{2} \qquad (2)$$

$$D(Y)_k = \frac{n_k - n_{kk}}{2} \qquad (3)$$

3. RESULTS AND ANALYSIS

This section will present the results of this study. First, the land cover map for the entire American continent from Ellesmere Island to Tierra del Fuego will be presented and described. Another section will focus on a quantitative analysis of this map and a comparison to another existing map product for the American continent.

3.1. The America map

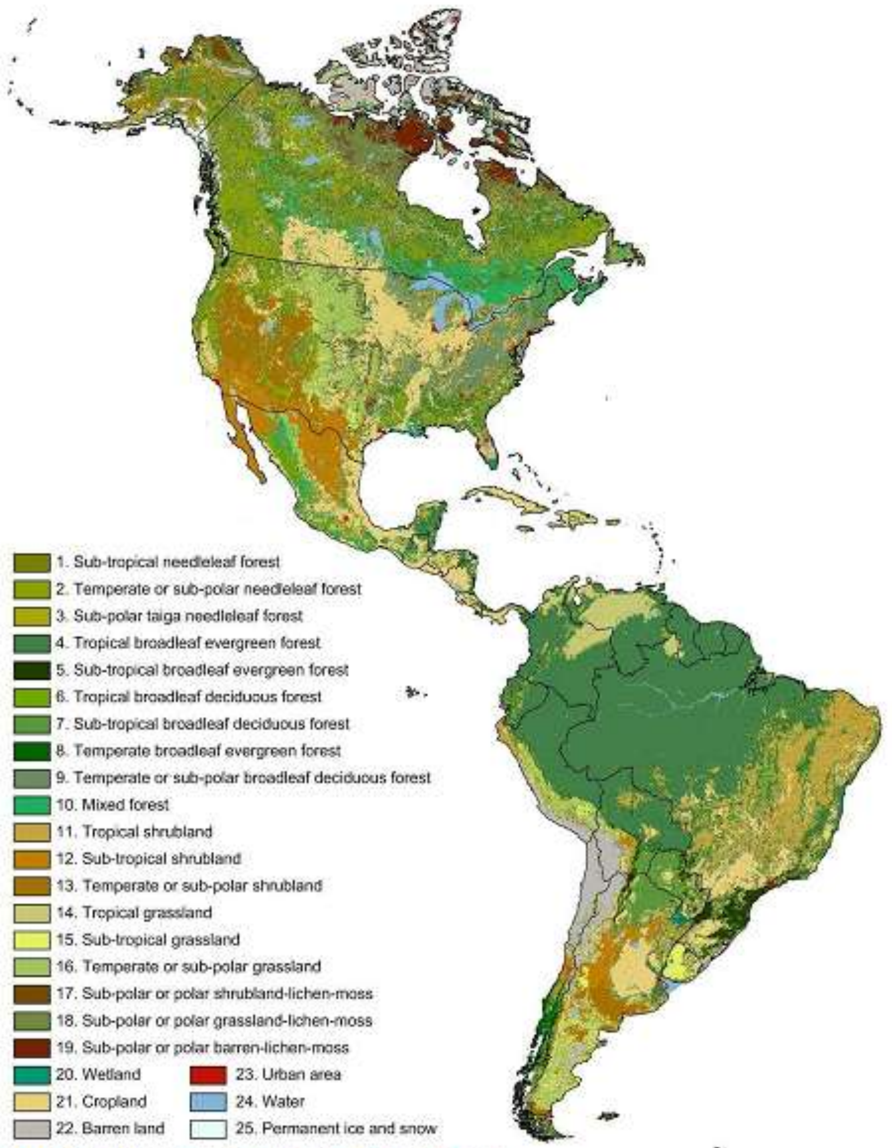

Figure 1. Land cover map of the American continent.

Figure 1. Land cover map of the American continent

Figure 1 presents the land cover map for the American continent. Zonal patterns dominate the northern parts of the North American continent. Meridianal mountainous systems like the Appalachians and the Western Cordilleras interrupt this pattern with broadleaf deciduous forests and shrubland in the semi-arid regions of the interior basins and Colorado plateau. Also, land use patterns become visible at a broad scale with cropland extending from Alberta and Saskatchewan to the southern United States East of the Mississippi/Missouri system. West of this system dominate temperate grasslands. Towards Mexico those classes change towards their tropical-subtropical counterparts with temperate classes continuing towards the South at higher elevations. Other Central American countries are dominated by cropland that intermingles with tropical and sub-tropical forests. South America is dominated by the tropical broadleaf evergreen forests in the Amazon basin that extent towards the Atlantic coast with transitions to tropical shrubland and sub-tropical forests. Climatic gradients are clearly visible for South America's lowlands, changing from tropical to sub-tropical and eventually to temperate classes in Patagonia. Also the hypsometric gradient can be easily observed for land cover classes in the Andean ranges. Latifovic et al. (2012) and Blanco et al. (2012) describe in more detail and quantitative fashion the land cover for North America and Latin America, respectively, and Colditz et al. (2012) with even more detail for Mexico.

3.2. Quantitative map comparison

For quantitative map comparison the North American map was aggregated to 12 basic land cover classes. The specific aggregation scheme is presented in Table 1. This generalized map was compared to the MODIS land cover product for the year 2005 with 17 classes following the IGBP legend (Friedl et al. 2002, Friedl et al. 2010).

The MODIS product was obtained in tiles that were mosaicked for entire America and projected to the same LAEA parameters and grid as the America map.

The aggregation rules of the MCD12Q1 product with 500m spatial resolution was not straight-forward and followed specific semantic and spatial rules that are also summarized in Table 1.

Figure 2 presents the quantitative class-wise comparison between the generalized America and MCD12 IGBP map. Coniferous forest that mainly exists in Canada, the United States and higher elevations for the rest of the study area shows a good agreement of 62%. There is a proportion of 25% that was only mapped in MOD12 IGBP but not in America and a proportion of 13% vice versa. The agreement was even better for broadleaf forest with 94%. Even more important is that this class makes up a large part of the land surface with approximately 28% of the total area. In this light one has to see the poor agreement of mixed forest (35%) because less than 4% of the total land corresponds to this diverse class that is hard to define and only exists in North and Central America. Another spatially important class is shrubland with approximately 16% of the total land surface. This class shows good correspondences above 70%. Grassland indicates lower agreements with only slightly above 50%. The larger disagreement occurs for the MOD12 IGBP map with 33% because this map classified more grassland than the America map. Lichen and moss only exists in the northern zones of North America and shows good general agreements above 70%. Although having poor agreements (23%) this number for wetland has only a limited importance because of its small area proportion over the entire study area (approximately 2%). In contrast, cropland with a share between 11 and 15% of the area is rather important. The agreement of 70% is moderate due to more mapped cropland in America than in the MOD12 IGBP map. Other classes (barren land, urban and built-up, water, snow and ice) show moderate to poor agreements but their importance in terms of total area is low.

Table 1. Aggregation of the America map legend and the MCD12 IGBP legend to a generalized 12-class legend.

General land cover classes	America map	MCD12 IGBP
1. Needleleaf forest	1. Sub-tropical needleleaf forest, 2. Temperate or sub-polar needleleaf forest, 3. Sub-polar taiga needleleaf forest	1. Evergreen needleleaf forest, 3. Deciduous needleleaf forest, 8. Woody savanna
2. Broadleaf forest	4. Tropical broadleaf evergreen forest, 5. Sub-tropical broadleaf evergreen forest, 6. Tropical broadleaf deciduous forest, 7. Sub-tropical broadleaf deciduous forest, 8. Temperate broadleaf evergreen forest, 9. Temperate or sub-polar broadleaf deciduous forest	2. Evergreen broadleaf forest, 4. Deciduous broadleaf forest, 8. Woody savanna, 9. Savanna, 14. Cropland / natural vegetation mosaic
3. Mixed forest	10. Mixed forest	5. Mixed forest
4. Shrubland	11. Tropical shrubland, 12. Sub-tropical shrubland, 13. Temperate or sub-polar shrubland	6. Closed shrublands, 7. Open shrublands, 8. Woody savanna, 9. Savanna, 14. Cropland / natural vegetation mosaic
5. Grassland	14. Tropical grassland, 15. Sub-tropical grassland, 16. Temperate or sub-polar grassland	8. Woody savanna, 9. Savanna, 10. Grasslands, 14. Cropland / natural vegetation mosaic
6. Lichen and moss	17. Sub-polar or polar shrubland-lichen-moss, 18. Sub-polar or polar grassland-lichen-moss, 19. Sub-polar or polar barren-lichen-moss	7. Open shrublands
7. Wetland	20. Wetland	11. Permanent wetlands
8. Cropland	21. Cropland	12. Croplands, 14. Cropland / natural vegetation mosaic
9. Barren land	22. Barren land	7. Open shrublands, 16. Barren or sparsely vegetated
10. Urban and built-up	23. Urban area	13. Urban and built-up
11. Water	24. Water	0. Water
12. Snow and ice	25. Permanent ice and snow	15. Snow and ice

Note: Some classes of the MCD12 IGBP map correspond to multiple land cover classes in the generalized legend. In this case spatial rules were applied, i.e. this class was converted to a specific general land cover class if it corresponded to the label.

An interesting number can be presented if the generalized 12 classes are combined to 3 basic classes that are forest (coniferous, broadleaf and mixed forest), natural vegetation (shrubland, grassland, lichen and moss, and wetland) and other (remaining classes). For forest the agreement is 90%, for natural vegetation 81%, and for all other classes combined 76%. For the map overall, the agreement is 72%.

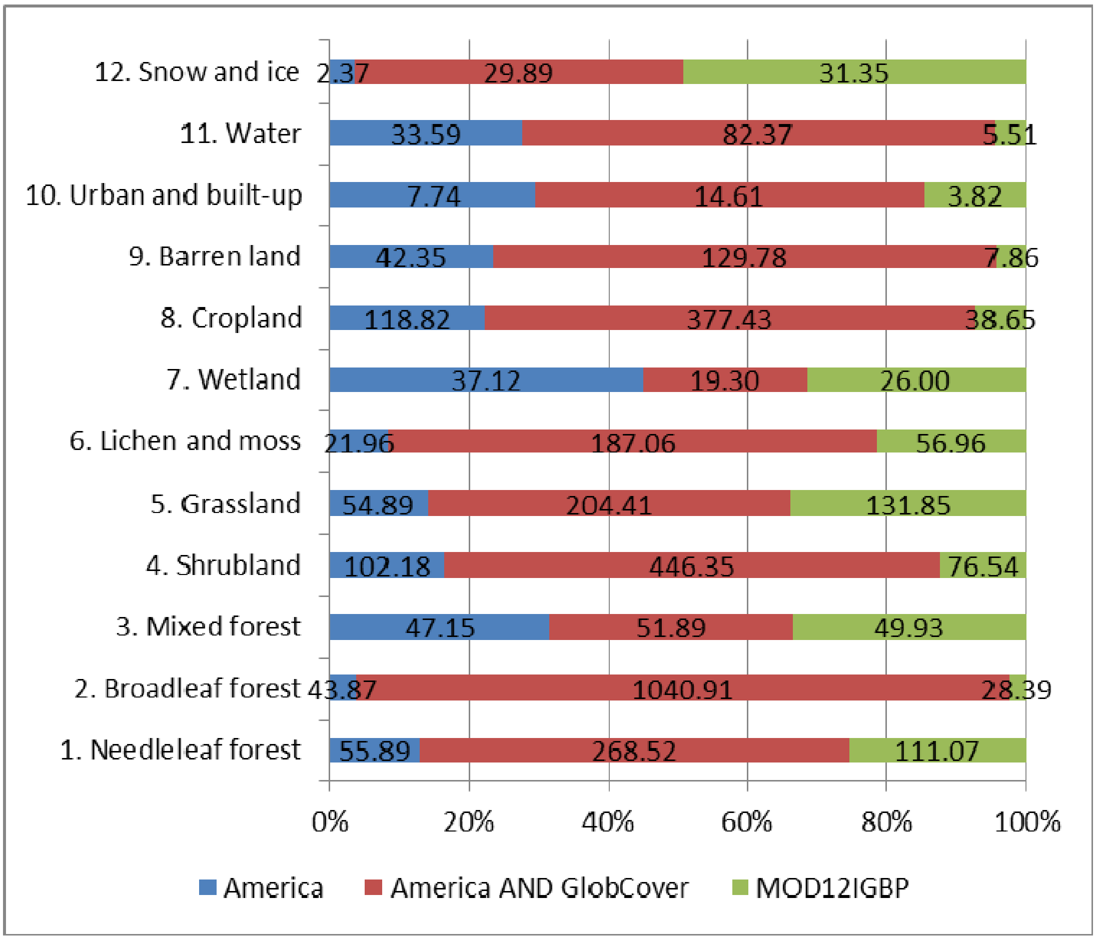

Figure 2. Class-specific agreement and disagreement (in per cent and Mio ha) between the America and MDD12 IGBP maps with generalized legends (see Table 1)

4. CONCLUSIONS

The paper presented the generation of a land cover map for the entire American continent. Due to the similarities between the NALMCS and SERENA project such a map can be accomplished by only a few processing steps. The map is important for projection on the continental scale such as climate modeling and species distribution and migration studies. The map is similar to other existing products with the advantage of presenting more thematic classes than several other products.

REFERENCES

Blanco, P.D.; Colditz, R.R.; López Saldaña, G.; Hardtke, L.A.; Llamas, R.M.; Mari, N.A.; de los Angeles Fischer, M.; Caride, C.; Aceñolaza, P.G.; del Valle, H.F.; Lillo-Saavedra, M.; Coronato, F.R.; Opazo, S.A.; Morelli, F.; Anaya, J.A.; Sione, W.F.; Zamboni, P.; Barrena Arroyo, V. A new land cover map of Latin America and the Caribbean in the framework of SERENA Project (RedLaTIF - GOFC-GOLD). Remote Sensing of Environment, submitted, 2012.

CEC. http://www.cec.org/ 2010.

Colditz, R.R.; Schmidt, M.; Conrad, C.; Hansen, M.C.; Dech, S. Land cover classification with coarse spatial resolution data to derive continuous and discrete maps for complex regions. Remote Sensing of Environment, vol. 115, p. 3264-3275, 2011.

Colditz, R. R.; López Saldaña, G.; Maeda, P.; Argumedo Espinoza, J.; Meneses Tovar, C.; Victoria Hernández, A.; Zermeño Benítez, C.; Cruz López, I.; Ressl, R. Generation and analysis of the 2005 land cover map for Mexico using 250 m MODIS data. Remote Sensing of Environment, vol. 123, p. 541–552, 2012.

di Gregorio, A. Land cover classification system—classification concepts and user manual for software version 2. FAO Environment and Natural Resources Service Series, No. 8, Rome, 2005, 208 p.

Fisher, P.; Comber, A.; Wadsworth, R. Land use and land cover: contradiction or complement. In Fisher, P.; Unwin, D.J. (Org.). Re-Presenting GIS, Chichester, John Wiley and Sons, 2005, p. 85-98.

Friedl, M.A.; McIver, D.K.; Hodges, J.C.F.; Zhang, X.Y.; Muchoney, D.; Strahler, A.H.; Woodcock, C.E.; Gopal, S.; Schneider, A.; Cooper, A.; Baccini, A.; Gao, F.; Schaaf, C.B. Global land cover mapping from MODIS: algorithms and early results. Remote Sensing of Environment, vol. 83, no.1-2, p. 287-302, 2002.

Friedl, M.A.; Sulla-Menashe, D.; Tan, B.; Schneider, A.; Ramankutty, N.; Sibley, A.; Huang, X. MODIS Collection 5 global land cover: Algorithm refinements and characterization of new datasets. Remote Sensing of Environment, vol. 114, p. 168-182, 2010.

Latifovic, R.; Homer, C.; Ressl, R.; Pouliot, D.; Hossain, S.N.; Colditz, R.R.; Olthof, I.; Giri, C.; Victoria, A. North American land-change monitoring system. In C. P. Giri (Org.). Remote Sensing of Land Use and Land Cover: Principles and Applications, Boca Raton, Fl: CRC/Taylor & Francis 2012, p. 303-324.

Quinlan, J. R. C4.5: Programs for Machine Learning. San Mateo, CA, Morgan Kaufmann, 19

Development of an operational system for monitoring forest cover at national scale in 1990, 2000 and 2010

Louis-Vincent Fichet 1 and Christophe Sannier 2

1. Système d'Information à Référence Spatiale,
BP 59650 Villeneuve d'Ascq, France
2 Système d'Information à Référence Spatiale, BP 59650 Villeneuve d'Ascq, France
louis-vincent.fichet@sirs-fr.com

ABSTRACT

Tropical deforestation is today considered as a major environmental issue. And it is accepted that deforestation and forest degradation are estimated to contribute to about 7 to 15 % of the total greenhouse gas emissions. A post-Kyoto protocol mechanism was developed, termed the Reduction of Emissions from Deforestation and forest Degradation (REDD+). The development of deforestation monitoring systems and determination of historical trends for forest cover change are key point in the establishment of national or sub- national carbon policy. This paper aim to show how through three different projects, and four different countries, a single standardized methodology has been developed and applied to monitor forest cover in 1990, 2000 and 2010. Each of those projects (project GSE FM REDD in Gabon funded by the European Spatial Agency, REDDAF in CAR and Cameroon funded by the European Commission and SLCS in Bolivia funded by the CNES) aim to make an inventory of forest areas at national or sub-national scale in order to take stock of the forest cover changes over the past 20 years. The proposed services will form the basis of a wall-to-wall regional- wide forest cover monitoring in this four countries. Therefore, a new and cost efficiency methodology was set up in order to automatically map forest cover using only optical data.

Keywords: Remote Sensing, Image Processing, Forest monitoring.

1. INTRODUCTION

Tropical deforestation is today considered as a major environmental issue Justice et al. (2001), Zhang et al. (2005), Hansen et al. (2008). Deforestation and forest degradation are estimated to contribute to about 7 to 15 % of the total greenhouse gas emissions Achard et al. (2007), GOFC-COLD (2011). A post-Kyoto protocol mechanism was developed, termed the Reduction of Emissions from Deforestation and forest Degradation (REDD) and initiated at the UNFCCC Conference of Parties (COP) 11 in Montreal in 2005. One of the fundamental requirements in the UNFCCC process is the establishment of robust and transparent national forest monitoring systems. Moreover determination of historical trends for forest cover change is also a fundamental input in the establishment of national or sub-national policy in relation to REDD.
Land cover maps fulfill several functions in monitoring forest cover change. Firstly, they serve as a reference baseline against which future change can be assessed. Secondly, they help establish forest areas that need to be monitored for change. When using a land cover map to assess future change, consistent methodology and spatial resolution are critical for the interpretation of results Achard et al., (2007). Different methods are appropriate and reliable for forest cover mapping or monitoring at regional or national scales using remote sensing data. An approach using spatially explicit land conversion information derived from sampling.

Bodart et al., (2009) or wall-to-wall mapping techniques is considered the most appriate (GOFC-COLD, 2011).
Herein, a standardized method for monitoring forest cover and forest cover change from optical Earth observation data was developed and applied over significant areas in four separate countries listed in table 1.

Table1. Forest cover mapping project undertaken by sirs

country	Project	Funded by	user	Area
Bolivia (Pando)	SLCS Carbone	CNES	COINACAPA	63 000 KM²
Gabon (1/3 country in 2010)	GSEFM REDD	ESA	AGEOS	267 000 KM²
Central African Republic (Sangha Mbaéré, Lobaye and Ombella-M'Poko)	REDDAF	EU Commission	MEE RCA	87 000 KM²
Cameroon (Central Province)	REDDAF	EU Commission	MEE CAMEROON	90 000 KM²

The estimation of deforestation is a function of the forest definition, in the absence of national forest definition; the service will comply with FAO forest definition IPCC (2006), which provides a range of values from which countries can select their forest definition. Forest should be an area of minimum 1 ha, with a minimum tree crown cover (or equivalent stocking level) of 30% and a minimum tree height at maturity of 5m.
The proposed services will form the basis of a wall-to-wall regional-wide forest cover monitoring. Therefore, a new and cost efficiency methodology was set up in order to automatically map forest cover using only optical data. Technical specifications of forest area maps and forest cover change maps for 1990, 2000 and 2010 are listed in table 2.

Table 2.Forest Cover Maps 1990, 2000, 2010 and Forest Cover Change Maps 1990-2000 and 2000-2010 product specifications

Forest cover		*forest cover change map*	
Criteria	**Specification**	**Criteria**	**Specification**
Geometric accuracy	Around 30 meters	Geometric accuracy	Around 30 meters
Reference system	WGS 1984 UTM	Reference system	WGS 1984 UTM
Image quality	30 metres	Image quality	30 metres
Image acquisition	+/- 3 years	Image acquisition	+/- 3 years
Minimum mapping unit	1 ha	Minimum mapping unit	1 ha
Map classes	Forest / Non Forest	Map classes	IPCC
Thematic accuracy	85% +/- 5%	Thematic accuracy	85% +/- 5%

In Gabon, the ESA GSE FM REDD extension project aims at developing a pre- operational system for monitoring forest cover within the REDD framework. The activities in Gabon are coordinated by SIRS and the overall project by GAF AG. The Gabonese Agency for Space Studies and Observations (AGEOS) was set up in 2010 with the aim to establish a national infrastructure for environmental monitoring and preventing the impacts of climate change. One of the objectives of the AGEOS is to develop its capacity to monitor forest cover at national level. The Gabonese authorities see the GSE FM REDD project as a precursor to the establishment of such national forest monitoring system.
In Bolivia, the main aim of the SLCS project funded by the CNES and coordinated by SIRS is to develop a monitoring system to facilitate access to payment for environmental services by local fair-trade organizations involved in agroforestry

and deforestation avoidance projects. The case study in the Pando district in Bolivia has been developed in partnership with an organization of producers of Brazil nuts (COINACAPA). These nuts are not cultivated but harvested in the Amazon rainforest. This case study aims to show that it is an activity that contributes to preserving forest resources in the area in which they operate.

Finally, the FP7 REDDAF project coordinated by GAF AG, seeks to develop and implement improved methodologies for assessing activity data and emission factors which are key input data for carbon accounting in the REDD process. The improved methodologies support the development of operational service chains for forest monitoring. Two demonstration areas were selected to develop and implement these methodologies, one in Central African Republic (Sangha Mbaéré, Lobaye and Ombella-M'Poko) and a second in Cameroon (Central Province). Both service providers SIRS and GAF AG were involved in the production of the map products to further demonstrate the interoperability of the mapping service developed.

2. METHODOLOGY

The Forest Cover Map (Forest/Non-Forest map) generation is based on Optical imagery and the overall production process follows a stepwise approach.

2.1 Data source

The production of the forest cover and forest cover change maps were exclusively based high resolution Optical data. For the four study area, in 1990 and 2000, Landsat data appears to be the most suitable data for historical mapping: datasets are freely available (USGS), the satellite has a repetitivity of 16 days and the spatial resolution meets the services 'criteria (cf. table 1) Thus, Landsat TM 4 and TM 5 were used for 1990 and Landsat 7 ETM+ for 2000. For 2010, in Gabon, a combination of Landsat 7 ETM+ SLC off and ASTER data were used, in Pando (Bolivia) only Landsat 7 ETM+ SLC off were used. In CAR and Cameroon, a mix of RapidEye and Deimos data were used. Due to the heavy cloud cover conditions generally experienced over tropical area, several images were required to cover a scene entirely. It was almost always possible to acquire the imagery within the required time interval (i.e. +/- 3years from the reference year).

2.2 Pre-Processing

All data acquired were already georeferenced by the provider to an UTM projection. Theimage-to-image registration was performed using Landsat GLS-1990/2000/2005 as reference dataset Gutman *et al*. (2008). All input dataset was initially checked visually and a minimum set of 10 evenly distributed check points were selected to assess the quality of the registration. In cases when the computed RMS exceeded 30m, the image was rectified using a first order polynomial model. All were resampled to an output pixel size of 30m to create a consistent dataset for change detection. Finally a topographic normalization was applied for each image.

A cloud detection algorithm was developed based on the combination of an unsupervised classification approach combined with a visual comparison of the results with the input image to determine the threshold between cloudy and non-cloudy pixels. A cloud mask was produced for each input image to derive cloud cover statistics and to determine the effective coverage. Gap stripe on Landsat 7 ETM+ SLC off were processed as cloud area and thus were masked and considered as no data area.

2.3 Thematic Processing

Depending on statistical results of data covers calculations for each reference years (1990,2000 and 2010), the reference year getting the best coverage of data is chosen as time 0 (*t0*). *t0* was selected as it provided the most complete and homogeneous image coverage will be used as the basis of classification forest / non-forest. For forest cover map and forest cover change map in Gabon and Bolivia, *t0* correspond to the reference year 2000, in CAR and Cameroon, *t0* correspond to reference year 2010.

In a first step, the segmentation and classification of EO dataset from *t0* was carried out, followed by manual/visual enhancements of the classified Forest Cover Map. The derived classified map product from *t0* and the Landsat data from *t1* are used to derive the Forest Cover Map for *t1* and the Forest Cover Change Map *t0/t1* (classified into IPCC compliant Land Use classes). The *t0* or *t1* Forest Cover Map and the current EO data set from *t2* are then the basis to derive the Forest Cover Map from *t2* and the respective mapped Forest Cover Changes. A more detailed description of the single processing step is outlined in the following paragraphs.

2.3.1 Semi-Automatic Classification of Forest Cover and Segmentation Process

The classification of the area of interest into Forest & Non-Forest was performed for each cloud and cloud shadow masked image, by using the ERDAS Imagine software. Optical data from *t0* were used as input. An unsupervised classification of the area of interest was conducted with a large number of spectral classes to ensure a good representation of the thematic classes' variability. An interactive comparison of the classified image was performed to label each spectral class according to the Forest/ Non Forest thematic classes. A post- processing classification routine was applied to vectorise the results and eliminate polygons smaller than 1 ha.

2.3.2 Manual Post-Processing

Subsequent to the automated classification, an intensive interactive post-processing was applied. Areas incorrectly classified were relabelled. The manual post-processing was performed using in house developed tools built on the ESRI software suite, especially designed for this type of activity. Additional information sources (e.g. topographic maps) can be used to support this interpretation. In case of discrepancies between the ancillary data sources and the satellite images, the most up-to-date information from the satellite imagery was used.

2.3.3 Detection of Forest Cover Changes

The *t0* Forest Cover Map was used as a Mask with the *t1* imagery to identify areas of change. The geometry of the *t0* map was kept when no change was detected to avoid the creation of artefacts. This process was repeated for *t2*. The detected change areas identified as part of the *t1* and *t2* Forest Cover Map production process were classified into cropland, grassland, wetland, settlement or other land use which are IPCC compliant.

2.4 Accuracy assessment of classification results

As shown in Table 1, the thematic accuracy should reach 90%. Many methodologies to assess the accuracy of a map have been developed Stehman, (2009), Czaplewski et al, (2004), Czaplewski (2003), Congalton, (2001), (1999), (1991). The main objectives of the implementation of the thematic map accuracy assessment procedure are to provide objective unbiased information on the map accuracy, and a cost-efficient and well accepted procedure. The easiest way to ensure that a sample is unbiased is to select each element randomly Stehman and Czaplewski, (1998**).** Despite the fact that, random selection is completely unbiased, it can leave some areas uncovered resulting in a non-fully representative sample. Therefore, a good alternative is a combination of systematic and random approach resulting in a randomly unaligned systematic sample scheme shown in figure 1 Czaplewski et al, (2004), Stehman and Czaplewski, (1998). It consist in a systematic grid of 20 by 20 km cell within a single sample of 2 by 2 km is randomly selected. Each segment was photo-interpreted by a qualified photo-interpreter independent from the production team. Then 50 points are randomly selected in each sanple. A confusion or error matrix is usually produced Congalton, (1991) based on a comparison of single points on the maps. The overall classification accuracy can be calculated together with user's and producer's accuracies which represent respectively errors of omission and commission. This approach is particularly suited for the Forest Cover and Cover Change Map products.

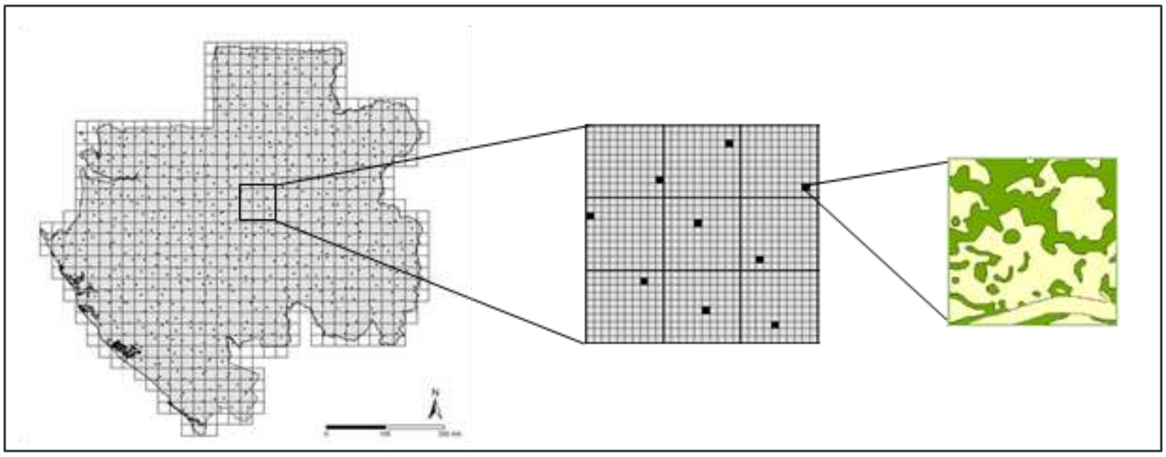

Figure 1. Illustration of the unaligned systematic sampling strategy over Gabon

3. RESULTS

Table 2 show initial results of forest cover by project and the table 3 the associated overall accuracy by reference year. In Cameroon results must be confirmed by the improvements of the dry-forest classification, it will be done during the phase 2 of REDDAF. Table 3 resume the deforestation rate by project and confirm the generally low level of deforestation in these four regions and in Gabon and Cameroon in particular.

Table 2. Forest covers for 1990, 2000 and 2010

	GABON	CAMEROON	CAR	BOLIVIE
1990	89.88%	73.14%	66.56%	96.40%
2000	89.64%	72.92%	65.56%	95.80%
2010	86.13%*	74,14%	64.03%	94.40%

* Deforestation rate for Gabon for a third of the country (102 000km²)

Table 3. Overall accuracy for 1990, 2000 and 2010

	GABON	CAMEROON	CAR	BOLIVIE
Overall accuracy 1990	98.8%	95.05%	90.1%	98.2%
Overall accuracy 2000	97.9%	95.18%	89.9%	97.7%
Overall accuracy 2010	97.4%	96.47%	91.6%	97.3%

Table 4. Deforestation rate by country for 1990/2000, 2000/2010 and 1990/2010

	GABON	CAMEROON	CAR	BOLIVIE
1990/2000	0.26%[1] 0.20%[2]	0.22%	1.5%	0
2000/2010	0.04%[2]	-0.52%[3]	0.8%	1
1990/2010	0.24%[2]	-0.30%[3]	2.3%	2

[1] Deforestation rate for Gabon between 1990 and 2000 are for the whole country (267 000km²)

[2] Deforestation rate for Gabon for a third of the country (102 000km²)

[3] The change results between 2000 and 2010 seem to overestimate the increase in forest areas due to misclassification of Dry Forest areas in the Centre Province of Cameroon. In phase 2 of REDDAF, the Dry Forest thematic will be more investigated to improve the overall results of the Deforestation mapping.

4. CONCLUSIONS

It was shown that it was possible to make wall to wall forest cover map at three time period at national or sub national scale using only optical data in tropical area known forheavy cloud cover, especially in Gabon. The maps produced are fully compliant with the product specifications agreed at the beginning of the project with all the users. The results shown indicate that the methodology developed is applicable in a range of different environments. The examples of CAR and Cameroon illustrate that a homogenous forest cover map can be produced by two separate service providers. In addition, as it is based on relatively simple and robust methods, it can potentially be implemented by countries wanting to develop their own forest monitoring system in the framework of REDD. And at international level to produce standardized reference forest cover map.

ACKNOWLEDGEMENTS

We would like to acknowledge Hannes Ott and Gernot Raminger from GAF AG (Munich, Germany) as leader of the consortium REDDAF and for their participation in the forest map production in CAR and Cameroon.

REFERENCE

Achard F., DeFries R., Eva H., Hansen M., Mayaux P., and Stibig H-J., Pan-tropical monitoring of deforestation. Environmental Research Letter, Volume 2, Number 4, 11p, 2007

Bodart C., Beuchle R., Simonett D., Eva H., Raši R., Carboni S., Brink A.,. Stibig H.-J, Achard F., Mayaux P., Global Monitoring of Tropical Forest Cover Changes by Means of a Sample Approach and Object -based Classification of Multi-scene Landsat Imagery: Pre-processing and First Results. Proceedings of International Symposium on Remote Sensing of Environment (ISRSE) 33. Stresa, Italy, 17 April 2009

Congalton, R.G. A review of assessing the accuracy of classifications of remotely sensed data. Remote Sensing of Environment. 37: 35-46, 1991

Congalton, R.G., Green, K., Assessing the Accuracy of Remotely Sensed Data: Principles and Practices, Lweis Publishers, 1999.

Congalton, R.G., Accuracy assessment and validation of remotely sensed and other spatial information, International Journal of Wildland Fire, 2001, 10, 321–328, 2001.

Czaplewski, Raymond L. Chapter 5: Accuracy assessment of maps of forest condition: statistical design and methodological considerations, pp. 115-140. Remote Sensing of Forest Environments: Concepts and Case Studies. (Michael A. Wulder and Steven E. Franklin, Eds.) Kluwer Academic Publishers, Boston. 515p, 2003.

Czaplewski, R.L., McRoberts, R.E., Tomppo, E. Sample design. In: Andersson, K, Bhandari, N., Czaplewski, R., Hussin, Y., Janz, K., Kleinn, Ch.,Magnussen, S. McRoberts, R. Melin, Y. Persson, R. Reed, D. Sandewall, M., Ståhl, G., Thomson, A., Tomppo, E., Vanclay, J. Knowledge Reference for National Forest Assessments. Http://www.fao.org/forestry/NfaKnowledgeRef/en/ 2004

GOFC-GOLD, 2011, A sourcebook of methods and procedures for monitoring and reporting anthropogenic greenhouse gas emissions and removals caused by deforestation, gains and losses of carbon stocks in forest raining forests, and forestation. GOFC-GOLD Report version COP17-1, 203p, 2011

Gutman, G., R. Byrnes, J. Masek, S. Covington, C. Justice and S. Franks, R. Headley, Towards Monitoring Land-cover and Land-use Changes at a Global Scale: The Global Land Survey 2005, Photogrammetric Engineering & Remote Sensing, January 2008

Hansen M. C., Roy D. P., Lindquist E., Adusei B., Justice O. C., Alstatt A.. A method for integrating MODIS and Landsat data for systematic monitoring of forest cover change in the Congo Basin. Remote Sensing of Environment, 112, 2495-2513, 2008

IPCC 2006, IPCC Guidelines for National Greenhouse Gas Inventories, Volume 4 (Agriculture, Forestry and Other Land Use), National Greenhouse Gas Inventories Program, Eggleston H.S., Buendia L., Miwa K., Ngara T. and Tanabe K. (eds). Published: IGES, Japan, 2006

Justice C., Wilkie D., Zhang Q., Brunner J. , Donoghue C., Central African forests, carbon and climate change. CLIMATE RESEARCH Vol. 17: 229–246, 2001

Stehman S. V., Sampling designs for accuracy assessment of land cover, International Journal of Remote Sensing, Vol.30, No. 20, 20 October 2009, 5243-5272, 2009

Stehman S. V, Czaplewski, R.L., Design and Analysis for Thematic Map Accuracy Assessment: Fundamental Principles, Remote sensing of environment, 64: 331-334, 1998.

Zhang Q., Devers D., Desch A., Justice C., Townshend J., Mapping tropical deforestation in central Africa, Environmental Monitoring and Assessment 101: 69–83, 2008

Distribuição espacial e potencial risco de esquistossomose na Ilha do Mosqueiro, município de Belém, Pará, Brasil

Alba Lucia Ribeiro Raithy 1; Ricardo José de Paula Souza Guimarães 2; Glaubus V. N. Barreiros 2; Arthur Carneiro Bernardes 3; Andrea M. N. Moraes 1; Sonia Claudia Almeida Pinto 1; Sergio A. O. Malcher 1; Nelson G. Veiga 4 e Clea Nazaré Carneiro Bichara 1

1. Universidade do Estado do Pará - UEPA
Rua Perebebuí, 2623 - 66087-670 - Belém/PA, Brasil
2. Instituto Evandro Chagas - LabGeo/IEC/SVS/MS
3. Secretaria Municipal de Saúde - SESMA/PA
4. Universidade Federal Rural da Amazônia - UFRA
albaraithy@hotmail.com

ABSTRACT

Schistosomiasis caused by *Schistosoma mansoni* is a disease conditioned to the presence of snails of aquatic habits of the genus *Biomphalaria*. Since schistosomiasis is a disease determined in space and time by environmental variables, the Geographic Information System (GIS) and Remote Sensing (RS) are techniques for the identifying factors and defining areas of possible risk of schistosomiasis. The objective of this study was evaluate the using of GIS and RS to characterize the spatial distribution of schistosomiasis in Mosqueiro Island (MI) focusing on the construction of scenarios representing potential areas for the occurrence of the disease. *B. straminea* was the only species of *Biomphalaria* found in 20 breeding sites. They are located in eight census tracts, 4 sectors located in Southwest MI and 4 in the West part of the island. The West region has a greater precariousness in relation to sanitation than the Southwest part of the MI. The results using kernel showed that there are 4 clusters of *Biomphalaria*. They are situated in only one cluster in Southwest and 3 in West of MI. The satellite image showed that the agglomerate of the Southwest having a large area with possibility of urban expansion. The lack of basic sanitation to support the new possible urban areas added with the *Biomphalaria* presence can leads to faecal contamination of natural aquatic environments, resulting in new sources of schistosomiasis transmission. This study showed the importance of the use of GIS and RS to study the risk of schistosomiasis in the MI.

Palavras-chave: geographic information system, schistosomiasis, *Biomphalaria*, sistema de informações geográficas, esquistossomose, *Biomphalaria*

1. INTRODUÇÃO

A esquistossomose mansônica, conhecida popularmente como barriga d'água é uma doença parasitária de veiculação hídrica causada pelo *Schistosoma mansoni* que se aloja nas veias do sistema porta-hepático; tem o homem como seu hospedeiro definitivo e caramujos de água doce (*Gastropoda*, *Pulmonata*, *Planorbidae*) do gênero *Biomphalaria* como hospedeiros intermediários (Brasil, 2008).

É uma doença considerada de importância em saúde pública por estar intimamente relacionada às condições de pobreza, fluxo migratório, precariedade do saneamento básico, dentre outros fatores socioambientais. As manifestações clínicas da doença são muito variáveis e dependem da fase e dos mecanismos fisiopatogenéticos envolvidos (Bichara et al., 1997). Na fase inicial os

sintomas mais aparentes decorrem em geral da penetração de cercarias na pele o que pode resultar em um quadro clínico com manifestações pruriginosas chamado de dermatite cercariana. Já a fase crônica da doença pode-se apresentar várias formas: hepatointestinal, hepatoesplênica e neurológica.
No Brasil a esquistossomose foi introduzida com a importação de populações africanas em regime de escravidão em meados do século XVI para trabalhar nas plantações de cana-de-açúcar no nordeste brasileiro (Barreto, 1982). O país é considerado o principal foco das Américas, com uma estimativa de cerca de 6 milhões de indivíduos infectados e outros 25 milhões sob o risco de contrair a doença (Katz e Almeida, 2003). As regiões n rdeste e sudeste do Brasil concentram as áreas com endemicidade mais elevada.
Com o fim do regime de escravidão, houve um expressivo aumento no fluxo migratório interno, o que levou a expansão dos focos da doença para outras regiões até então indenes. A esquistossomose chegou a Amazônia impulsionada pelo ciclo econômico da borracha no final do século XIX. O primeiro registro da ocorrência na Amazônia foi feito por Lutz em 1919, no estado do Acre. Posteriormente, Davis (1934), Pará (1948) e outros observaram vários casos em Belém e outras localidades, sem, no entanto a comprovação de sua autoctonia, o que só veio a ocorrer de fato em 1951 quando da descoberta do primeiro foco de transmissão ativa feita por Machado e Martins (1951), no município de Fordlândia, localizado a margem direita do rio Tapajós. Posteriormente, foram identificados dois outros focos autóctones: um no atual município de Quatipuru descrito por Pessoa de Melo e Gueiros (1959), que permanece ativo até os dias atuais, e o outro no bairro do Reduto em Belém, descrito por Galvão (1968), tendo se expandido depois para outros bairros da capital paraense (Bichara et al., 1997).
De acordo com a lei municipal Nº 7682/94, os 71 bairros que integram o município de Belém estão distribuídos em oito Distritos Administrativos (DA), a saber: DABEL (Belém), DABEN (Benguí), DAENT (Entroncamento), DAGUA (Guamá), DAICO (Icoaraci), DASAC (Sacramenta), DAOUT (Outeiro) e DAMOS (Mosqueiro) (Belém, 1994), sendo que apenas duas destas áreas (DAOUT e DAMOS) são indenes para esquistossomose, muito embora já tenha sido registrada a presença do caramujo em vários bairros (Aeroporto, Chapéu Virado, Ariramba, Baia do Sol, Carananduba, Maracajá, Vila, Murubira, Paraíso e São Francisco), bem como casos importados da doença já foram notificados (Belém, 2008).
Como a esquistossomose é uma doença determinada no espaço e no tempo por variáveis socioambientais, o Sistema de Informação Geográfica (SIG) e o Sensoriamento Remoto (SR) são técnicas para identificar esses fatores e definir áreas de possível risco de esquistossomose. (Guimarães et al., 2009).
Neste contexto, faz-se de extrema importância o levantamento de dados que possam contribuir para um melhor conhecimento acerca da dinâmica de transmissão e do comportamento epidemiológico do agravo, os quais poderão ser incorporados como práticas de caráter preventivo junto às estratégias desenvolvidas pelo Programa de Saúde da Família (PSF).
O objetivo deste estudo foi avaliar o uso de SIG e SR para caracterizar a distribuição espacial da esquistossomose no Distrito Administrativo de Mosqueiro, Belém/PA com foco na construção de cenários que representam as áreas potenciais para a ocorrência da doença.

2. METODOLOGIA DE TRABALHO

O Distrito Administrativo de Mosqueiro (DAMOS) é uma ilha fluvial situada entre 01º03’ e 01º05’ latitude Sul e 48º29’ e 48º18` longitude Oeste (W) de Greenwich, distante apenas 44,5 km de Belém e ocupando uma área de aproximadamente 212 km^2 de extensão (Figura 1), sendo limitada a sudoeste pela Baia do Guajará, a oeste pela Baía de Santo Antônio, a noroeste pela Baía do Marajó, ao norte e nordeste pela Baía do Sol, ao sul pelo Furo do Maguari e a sudeste pelo Furo das Marinhas. Por conta de sua proximidade geográfica, a ilha demonstra uma identidade ambiental muito similar a Belém, com clima equatorial superúmido com médias de temperatura em torno de 27 ºC e pluviosidade de **2**.800 mm anuais (Furtado e Silva Jr, 2009). Apresenta uma população residente estimada emaproximadamente 27.000 habitantes (IBGE, 2010).

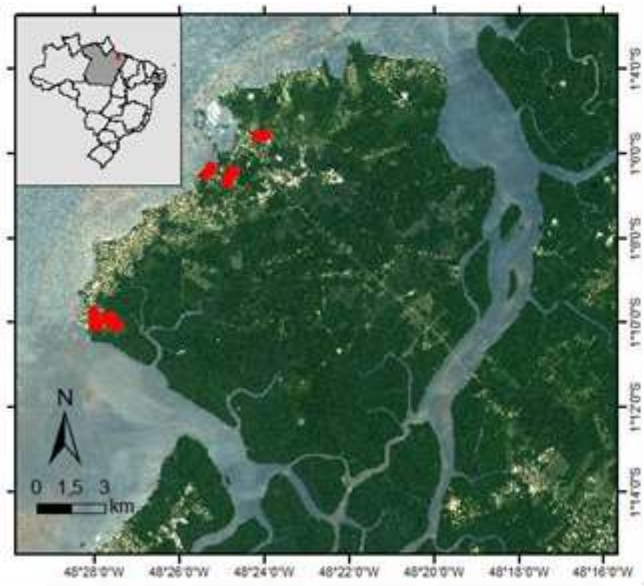

Figura 1. Ilha de Mosqueiro destacando em vermelho a localização espacial dos c
riadouros de caramujo *Biomphalaria*

Foi percorrida uma extensa área para demarcação e caracterização das coleções hídricas locais que apresentavam moluscos planorbídeos do gênero *Biomphalaria*, em parceria com os agentes comunitários de saúde (ACS) do Programa de Saúde da Família (PSF) envolvidos na pesquisa. A localização espacial dos 20 criadouros foi determinada através de um receptor GPS (*Global Positioning System*), como pode ser observado na Figura 1. As coordenadas dos criadouros foram comparadas com os dados dos setores censitários, obtidos do IBGE (Instituto Brasileiro de Geografia e Estatística).

Foi utilizado um Sistema de Informações Geográficas (SIG) para armazenar, organizar e analisar as imagens do satélite SPOT 5 e, também, para gerar um banco de dados.

Na construção dos mapas de superfície foi aplicado o kernel nos criadouros de *Biomphalaria*, segundo a metodologia descrita por Guimarães (2010). A largura de banda de 300 m foi utilizada para estimar a densidade do kernel dos criadouros. Os aglomerados obtidos com o kernel foram caracterizados com imagens do satélite SPOT 5.

3. RESULTADOS E DISCUSSÃO

Todos os bairros pesquisados do DAMOS apresentavam condições propícias para o desenvolvimento e proliferação dos caramujos, pois contavam com presença de corpos hídricos com baixa mobilidade de água, abundância de vegetação macrofítica e contaminação de valas e canais por matéria orgânica.

B. straminea foi a única espécie de *Biomphalaria* encontrada nos criadouros após a identificação morfológica. Porém, alguns exemplares serão submetidos à identificação por técnicas de biologia molecular (PCR) para confirmação da espécie. Caramujos de outros gêneros como *Physa* e *Pomacea*, embora não participem do ciclo de vida do *S. mansoni*, foram encontrados com bastante frequência nas áreas pesquisadas, algumas vezes dividindo o mesmo habitat com caramujos do gênero *Biomphalaria*.

Tabela 1. Setores censitários, bairros trabalhados, quantidade de criadouros (PT) e porcentagem de domicílios ligados à rede geral de água e esgoto

Setor	Bairro	PT	Residentes	Água	Esgoto
000001	Vila	2	1238	95,0	12,4
000002	Vila	1	637	89,7	29,7
000005	Maracajá	2	1033	95,0	31,7
000006	Maracajá	7	2312	90,7	5,7
000017	São Francisco	2	866	59,7	4,7
000022	Carananduba	1	1033	43,6	0,4
000024	Caruara	1	794	1,5	0,0
000035	São Francisco	4	1572	35,5	5,8

Todos os vinte pontos georreferenciados apresentaram coleções hídricas contendo criadouros. Eles estão situados em oito setores censitários, dois setores pertencem à localidade de Maracajá com nove criadouros, dois à Vila com três criadouros, ambos localizados no sudoeste da Ilha do Mosqueiro, e na parte oeste da ilha, existem dois setores pertencem à São Francisco com seis criadouros, dois à Carananduba com um criadouro e um à Caruara com um criadouro. A Tabela 1 mostra os oito setores censitários onde foram encontrados criadouros de caramujos *Biomphalaria*.

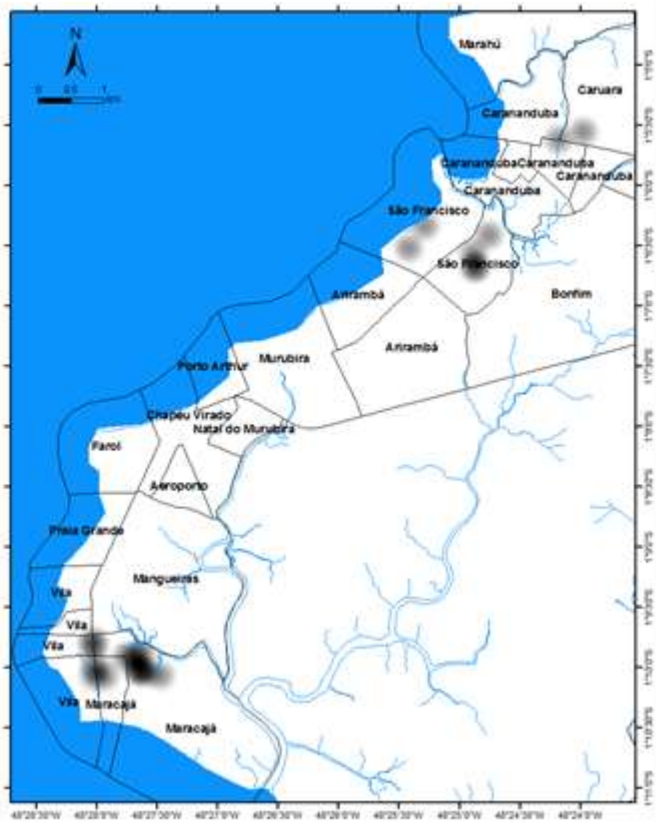

Figura 2. Aglomerados de criadouros de *Biomphalaria* resultantes da aplicação do kernel

Podemos observar na Tabela 1 que a localidade de Maracajá apresenta 92,1% dos seus domicílios ligados a rede geral de água e 13,7% ligados a rede geral de esgoto. Vila tem 93,1% dos seus domicílios ligados a geral de esgoto. São Francisco tem 44,4% dos seus domicílios ligados a rede geral de água e 5,4% ligados a rede geral de esgoto. Caruara apresenta 1,5% dos seus domicílios ligados a rede geral de água e não tem rede geral de esgoto. Carananduba tem 43,6% dos seus rede geral de água e 18,7% ligados a rede domicílios ligados a rede geral de água e 0,4% ligados a rede geral de esgoto. Logo, os resultados da Tabela 1 mostram que a região oeste apresenta uma maior precariedade em relação ao saneamento, do que à parte sudoeste da Ilha de Mosqueiro.

Figura 3. Aglomerados de criadouros de *Biomphalaria* com a imagem de satélite

O resultado utilizando o kernel apresentado na Figura 2 mostra quatro aglomerados de criadouros de *Biomphalaria*. Um aglomerado na região sudoeste e três na região oeste.
Na Figura 3 a imagem de satélite mostrou que o aglomerado da região sudoeste (Figura 3A) apresenta uma maior quantidade de residências do que da região oeste (Figuras 3B, C e D), principalmente no aglomerado de Caruara (Figura 3B) que apresenta uma área com grande possibilidade de expansão residencial.

4. CONCLUSÕES

Este estudo mostrou a importância da utilização de Sistemas de Informações Geográficas (SIG) e Sensoriamento Remoto para estudar o risco de esquistossomose na Ilha do Mosqueiro, Guimarães et al. (2010) usou SIG para estudar e controlar a esquistossomose em Minas Gerais.
Embora não tenha sido encontrada qualquer *Biomphalaria* infectado, existe relato de moradores com esquistossomose não autóctone na área de estudo. Além disso, os resultados mostram que a região oeste da Ilha de Mosqueiro apresenta um alto potencial para a instalação de focos de transmissão da esquistossomose, pois exibem coleções hídricas com população intensa de caramujos vetores, precariedade do sistema de esgotamento sanitário, deficiência na distribuição de água tratada, dentre outros fatores.
É importante salientar que o DAMOS passa por um processo de ocupação desordenada de seu espaço, com intenso fluxo migratório de famílias numerosas que se deslocam para locais que não dispõem de estrutura básica de moradia, oriundos principalmente de municípios vizinhos como Santa Bárbara e Santo Antônio do Tauá, bem como de outras regiões do país. Destacando os migrantes da região nordeste (área endêmica de esquistossomose) que vem em busca de melhores oportunidades de trabalho, mas que em virtude de baixa escolaridade acabam por engessar a massa de desempregados, que acabam por invadir áreas de matas primárias, localizadas em geral próximas a mananciais. Por isso, devido às atividades antrópicas, os mananciais tornam-se poluídos, e aliados a isto, temos ainda um crescimento populacional desordenado de maneira que o sistema de saúde local não tem como atender toda a população, contribuindo para o aumento da incidência de várias doenças infecto parasitárias.
Peixoto e Machado (2005) e Anaruma Filho e Santos (2007) no estudo da esquistossomose na Usina Hidrelétrica de Miranda/MG e Campinas/SP mostram os mesmos fatores apresentados nesse estudo, relacionados aos problemas socioambientais, econômicos e de falta de serviços essenciais de saneamento básico e água tratada.
A área de risco para a esquistossomose foi obtida pelo estimador de kernel que identificou os locais através dos aglomerados e, também, foi possível calcular, utilizando um SIG, a sua extensão e com o auxilio de uma imagem de satélite determinar as características ambientais da área do aglomerado. Cardim et al. (2011) identificou áreas de risco para a esquistossomose em Lauro de Freitas/BA usando dados socioambientais, epidemiológicos e estimador kernel.

AGRADECIMENTOS

A Universidade do Estado do Pará (UEPA), Laboratório de Geoprocessamento do Instituto Evandro Chagas (LabGeo/IEC), Secretaria Municipal de Saúde (SESMA), Núcleo de Medicina Tropical da Universidade Federal do Pará (NMT/UFPA) e agentes comunitários de saúde do Programa de Saúde da Família (PSF).

REFERÊNCIAS BIBLIOGRÁFICAS

Anaruma Filho, F.; Santos, R.F. Indicadores da relação entre estrutura da paisagem, degradação ambiental e esquistossomose mansoni. In: Congresso de Ecologia do Brasil, 2007, Caxambu. Anais.São Paulo:SEB, 2007. Artigos, v.8, p. 1-2. On-line. <http://www.seb-ecologia.org.br/viiiceb/index1.html>. Acesso em: 03 out. de 2012.
Barreto, M. L. Esquistossomose Mansônica. Distribuição da Doença e Organização Social do Espaço. 1982. Dissertação de Mestrado - Departamento de Medicina Preventiva, Universidade Federal da Bahia, Salvador. 1982.
Belém, Prefeitura Municipal. Distritos administrativos do Município de Belém: Divisão Político- Administrativa. SEGEP - Secretaria Municipal de Coordenação Geral do Planejamento e Gestão. Belém: Diário Oficial (Conforme Lei N° 7.682 de 05 de Janeiro de 1994), 1994.
Belém. Secretaria Municipal de Saúde. Resumo anual das atividades de malacologia por localidade. Departamento de Vigilância à Saúde. Divisão de Controle de Endemias. Programa de Controle de Esquistossomose. Belém: 2008
Bichara, C.N.C; Soares, I.S.; Rodrigues, I.R.C. Esquistossomose Mansônica. *In*: Leão, R.N. Q.

L. (Coord). Doenças Infecciosas e Parasitárias: enfoque Amazônico. Belém, PA: Cejup, 1997. p. 687-699.
Cardim, L.L.; Ferraudo, A.S.; Pacheco, S.T.A.; Reis, R.B.; Silva, M.M.N.; Carneiro, D.D.M.T.; Bavia, M.E. Análises espaciais na identificação das áreas de risco para a esquistossomose mansônica no município de Lauro de Freitas, Bahia, Brasil. Cad Saúde Pública, v. 27, n. 5, p. 899-908, 2011.
Davis, N. C. The microscopical examination of 29,593 human livers from central and northern Brazil, with special reference to the occurrence of malaria and schistosomiasis. Amer. J. Hyg. v.19, n. 3, p. 567-600, 1934.
Felgueiras CA, Moura, A.C.M.;, Amaral, R.S.; Drummond, S.C.; Scholte, R.G.C.; Oliveira, G.C.; Carvalho, O.S. Spatial distribution of *Biomphalaria* mollusks at São Francisco River Basin, Minas Gerais, Brazil, using geostatistical procedures. Acta Trop, v. 109, n. 3, p. 181- 186, 2009.
Furtado, A.M.M. Silva Junior, O.C. Impactos Ambientais do Desmatamento e Expansão Urbana na Ilha do Mosqueiro. In: Encontro de Geógrafos da América Latina, 12, 2009, Montevidéu. Anais... Montevidéu:SGAM, 2009. Artigos, p. 1-2.
Galvão, S.S. Esquistossomose em Belém do Pará. Rev. Bras. Malariologia e Doenças Trop.. v. 20, n. 3-4, p. 215-223, 1968.
Guimarães, R.J.P.S. Ferramentas de geoprocessamento para o estudo e controle da esquistossomose no Estado de Minas Gerais. 2010. 226 p. Tese (Doutorado em Biomedicina) - Santa Casa de Belo Horizonte, Belo Horizonte, 2010.
IBGE (Instituto Brasileiro de Geografia e Estatística). Censo Demográfico 2010. Disponível em: <http://www.sidra.ibge.gov.br /bda/tabela/protabl.asp?c=137&z=t&o=7&i=P>. Acessado em: 03 out. de 2012.
Katz, N.; Almeida, K. Esquistossomose, xistosa, barriga d'água. Revista Ciência e Cultura. v.55, n. 1, p.38-43, 2003.
Machado, W.G.; Martins, C. Um foco autóctone de esquistossomose no Pará. Hospital, v. 39, n. 2: p. 289-290, 1951.
Pará, M. Schistosomose Mansônica no Brasil. Ocorrência em fígados de viscerotomia no período de 1937-1946. In: Congresso Brasileiro de Higiene, 7, 1948, São Paulo. Anais. São Paulo, 1948.
Peixoto, L.E.; Machado, M.I. Vigilância ambiental em saúde: ocorrência de *Biomphalaria peregrina* e *B. schrammi* em áreas de influência da usina hidrelétrica de Miranda, Minas Gerais. In: Congresso Brasileiro de Engenharia Sanitária e Ambiental, 23, 2005, Campo Grande. Anais... v. 23, p. 1-9, 2005. On-line.<http://www.bvsde.paho.org/bvsacd/abes23/ VII-051.pdf>. Acesso em: 19 abr. de 2009.
Pessoa de Melo, E; Gueiros, S. Novo foco de esquistossomose mansônica na Amazônica (Foco de Quatipuru – Mun. Capanema – Estado do Pará) setembro de 1957. In: Jornada Médica Paraense, 1, 1959. Capanema. Anais. Capanema, 1959.

Tracking mud-bank migration from remote sensing and in-situ data: The example of the Kourou River Estuary, French Guiana, South America

Christina Péron 1-2; Antoine Gardel 1-2; Andy Chatelet 2 and Erwan Gensac 2

1 CNRS Guyane, USR 3456, 2, avenue Gustave Charlery , 97300 Cayenne
2 Laboratoire d'Océanologie et Géosciences, UMR 8187, 2 avenue Foch, 62930 Wimereux
Christina.peron@univ-littoral.fr Antoine.gardel@univ-littoral.fr
Andy.chatelet@univ-littoral.fr, erwan.gensac@univ-littoral.fr

ABSTRACT

The special fine sediment dynamics on South America coastal environment under the influence of the Amazon river had been highly documented during the last decades. Thus, huge mudbanks migrate along thousand kilometers of coast until the Orinoco delta. These banks are constituted by an intertidal part formed by consolidated mud and with a subtidal area of the mudbank composed by fluid mud. The aim of this short paper is to combine remote sensing and in-situ measurement in the determination of mud bank migration both in the intertidal and subtidal area. The determination of the delimitation of the intertidal part of the bank are monitored using remote sensing images acquired at low water level. While the waves attenuation are used as a proxy of the subtidal part localization. In fact, waves are dampened by fluid mud at proximity of the subtidal area, and are highly detectable on SPOT images. Moreover, in-situ measurement in the Kourou river channel provide data of the fluidify mud on the channel from 2002 to 2012. It was observed that the passage of the mudbank contribute differently along the channel with a more pronounced arrival of fluid mud in the offshore part of the navigation channel between 2003 and 2009 while the onshore channel were silting-up by the trailing edge of the mudbank from the mid-2009. Combining both the mudbank position from remote sensing images analyses and mud lens survey allow the determination of the localization of a mudbank along the Kourou coast for 10 years.

Keywords: Intertidal, Subtidal, fluid mud, in-situ measurement, image Processing

1. INTRODUCTION

The Guianese coast is the muddiest shoreline of the world. These coasts experience important fine-grained sediment supply due to the Amazon river discharge (Augustinus, 1978). These cohesive sediments lead to the formation of huge mud banks which migrate along the Guianese coast (Froidefond et al.,1988;Gardel and Gratiot,2005;Anthony et al., 2010). Mudbank and associated mangroves-fringe shores form parts of the sea side environment along the 1600km from the Cabo Cassipore (Brazil) to the Orinoco river (Venezuela) (Augustinus et al., 2004, Warne et al., 2002). As a consequence of mudbanks migration, the shorelines are in perpetual fluctuations (Gardel and Gratiot, 2004; Anthony et al., 2010). The migration of these huge mudbanks (10 to 60km-long, 20 to 30km-wider and 5m-thick, Froidefond et al., 1988) could attain up to 5km by year (Gardel and Gratiot, 2005). This coast is organized in "bank" and in "interbank" phases(Anthony and Dolique,2004; Baghdadi et al.,2004). Bank phases consist of a prograded coast protected by wave action due to the important wave dampening on the mudbank offshore extension (Anthony et Dolique, 2004).

Bank phases lead to the installation of mudbank, and therefore a prograded coast from 20 to 30km shore to offshore, consolidation of mud engendered the development of a mangrove forest. Besides, these phases lead to coastal silting-up no matter the type of environment (sandy beach, rocky shore, harbor or harbor channel). As a contrary during “interbank” phases the coast is free of any protection against wave attack, and erosion of the colonized mudbank and shoreline are consequent. Mudbank are divided in several part, the first one consist of an intertidal part which is situated in the fluctuated tidal environment. This part is composed by consolidated mud created by fluid mud arrival through the action of coastal current. The subtidal part which is in permanent submerge are formed by fluidify mud, the waves are totally attenuated at their approach. The subtidal area of a mudbank constitutes the bigger part of the bank and therefore their migration represent a key in the migration processes. Several studies had been focused on intertidal mudbank migration (Froidefond et al., 1988, Gardel and Gratiot, 2004,2005) with the purpose of quantified the migration rates of a mudbank along interbank area. Nevertheless, any geomorphological studies had been devoted on the characterization of the subtidal part migration processes, which need important in-situ measurement such as seismic profiles and bathymetric survey.

The extreme coastal fluctuation along the French Guiana coast engendered important difficulties for coastal decision makers. A better knowledge of the integral mudbank migration processes is then a priority in order to have a better understanding of the rapid coastal changes. The aim of this paper is to integrate both data extracted from remote sensing analysis and in-situ measurement for tracking mud-bank migration.

2. METHODOLOGY

2.1 Study site

The study site is located on the Kourou coast, which comprised the Kourou river channel harbor (e.g .Figure 1). These coast suffer from important fluctuations due to the complex mudbank processes. Arrival of fluid mud on the coast leads to the modification of coastal bathymetric.

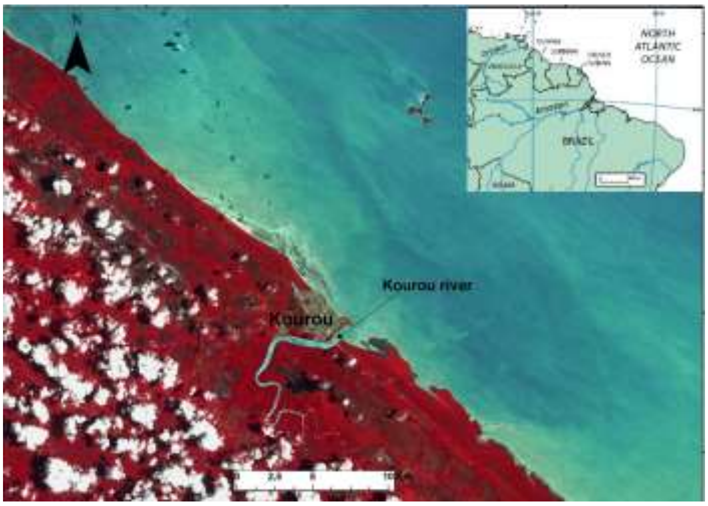

Figure 1. Satellite imagery (SPOT image, 30/09/2011, SEAS Guyane) of the Kourou coast and localization of the Kourou river

Along Kourou coast, arrival of mud cause a silting-up of the coastal environment and could lead to a silting-up of the Kourou river navigational channel, provoking the non-access of the river due to the high elevation of the bottom depth. Therefore, constant dredging are realized to evacuate the mud inside the channel, and to facilitate access of the navigational channel.

2.2. Remote sensing

To determine coastal change, multi-spectral and multi-temporal satellite images are used in the present study. Intertidal part of mudbank is clearly visible on satellite images when acquisition is realized at lower water level, whereas subtidal part could be delimited only by waves dampening. This type of data permits a geo-localization of mudbank on the Guianese coast. Satellite images are used to extract the position and area of the mudbank using a semi-automatic algorithm (e.g. Figure 2.A). This method regroups photo-interpretation and segmentation. The two-dimensional morphology of the mudbank is obtained at lower water- level.

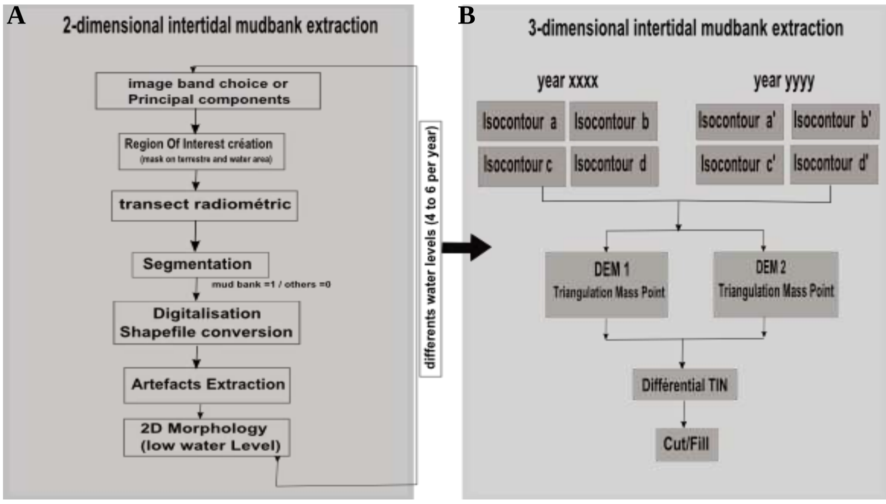

Figure 2. Extraction methodology: A/two-dimensional and B/three-dimensional morphology

The near infra-red (NIR), mid infra-red (MIR), red and green bands are used to extract the coastal features elements of our study: mangroves-fringe and mud.

The surface of intertidal part of mudbank depends on the water level as a consequence images acquired at different water-level allow the realization of three-dimensional mudbank morphology.

Therefore, the intertidal topography of a mud-bank is obtained by several isocontours acquired at different water level between low and high tide (e.g. Figure 3).

Two conditions are required for quality results: images acquired in a short-time interval (to analyze the same bank position) and a panel of images which cover the tidal amplitude (e.g. Figure 3). These data lead to the realization of a Digital Elevation Model (DEM) of the muddy bank.

The interval of altitude of the mud correspond to the interval between two isocontours. All images were in the world reference system(WGS 84) datum and were projected using the Universal Transverse Mercator system (zone UTM 22).

The subtidal part of the mudbank had been extracted by manual method on eight SPOT images in this study (14/10/2001, 02/11/2002, 15/09/2003, 25/06/2006, 24/09/2007, 02/07/2008, 16/10/2010, 26/10/2011).

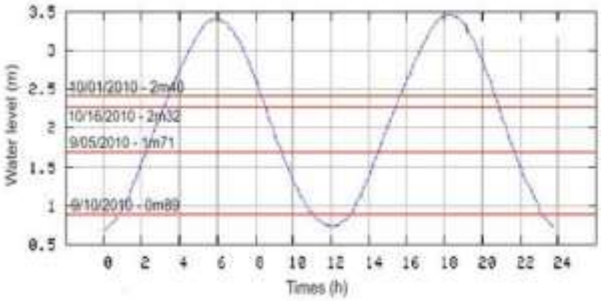

Date	Water Level	Satellite & Resolution
10/09/2010	0m89	SPOT 5 - 10 m
05/09/2010	1m71	SPOT 5 - 10 m
16/10/2010	2m32	SPOT 5 - 10 m
01/10/2010	2m40	SPOT 5 - 10 m

Figure 3. Chosen SPOT-5 images for the three-dimensional mudbank morphology
(Example of the mudbank of Kourou in 2010)

2.3. In situ measurement

From 2002, Atlantic Dragage society has been mandated by the Guianese Spacial Center with the purpose of prevents silting up of the Kourou river by monitoring the fluctuated channel depth. The data acquired during the bathymetric survey permit extraction of the mud lens thickness along the Kourou river channel (14-kilometers long) on particular point, named “Kilometric Point”(PK). The mud lens thickness is an indicator of the potential arrival of fresh fluid mud on the channel. The long-term analyze of the bottom thickness of the mud- lens gives temporal evolution and migration of the mudbank.

3. RESULTS AND DISCUSSION

3.1. Tracking mud-bank from remote sensing

Several methods are used for coastal environments monitoring of French Guiana. However, for a better knowledge of the coastal processes involved in the mudbank migration, we need the combination of remote sensing and in-situ measurement. The present study combined several approaches in order to evaluate the migration of a mudbank along the French Guiana coast. The migration of the huge mudbank along the coast modify the shore morphology through time.

The knowledge of their two and three-dimensional morphology and processes of migration are required to prevent or to predict and follow their movement.

In 2010, the two-dimensional morphology of the mudbank of Kourou (e.g. Figure 4A) is obtained between coastline (green line) and an isocontours acquired at a water level of 0.89m (red line). This low level had permitted to observe a huge surface of intertidal mudbank. A diachronic survey will permit to obtain two and three-dimensional deformations of the intertidal part of the mudbank using spatial indicator (e.g. Figure 4A and 4B).

In 2010, the DEM of the mudbank of Kourou(cf.fig.4) indicated lower altitude on the offshore part of the mudbank whereas the inner part is more concentrated in mud and therefore has higher altitude. Besides, we noted that the trailing and lee edge of the mudbank comprised lower altitude and therefore less mud than the middle part of the mudbank which attains up to 2m40.

The two and three-dimensional morphologies are used in order to define deformations: migration velocity (distance between two successive barycentre, AVB, or ARB), and altimetric deformations (difference between two DEM).

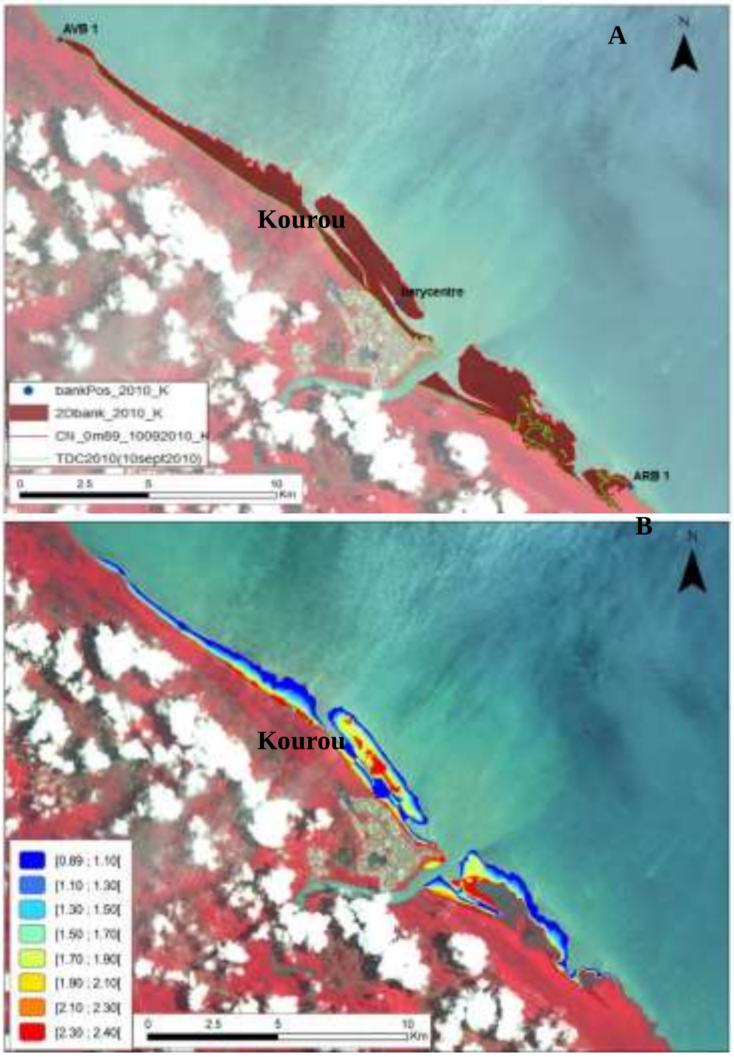

Figure 4: A/ Two-dimensional morphology defined by spatial indicators (front of mudbank (AVB), back of mudbank (ARB) and barycentre of mudbank). The intertidal mudbank is also characterized by and area which is defined between an isocontours acquired at low tide and coastline. B/ Three-dimensional morphology; result of a spatial interpolation, two main types of interpolation (kriging and triangulation method). (Images: SPOT-5 images from SEAS Guyane)

The analyze of the subtidal part indicated a northwestward migration and a deformation of the bank along the coast (e.g. Figure 5). The offshore limit of the bank is curved from the lee to the trailing edge. The recent subtidal delimitation (from 2006) after the passage of the Kourou river suggested a more larger subtidal part, facilitated by the arrival of recycling mud from the back to the front of the bank. This observation coincides with the previous one for the intertidal part of the mudbank. The subtidal delimitation of the mudbank gives the total cover area of the bank along the coast. If the bank position identification was realized only by the intertidal bank there will be a lack of data. In fact, by observing the subtidal delimitation in 2010 (e.g. Figure 5) and the intertidal area (e.g. Figure 4) we could denote that the intertidal bank represent a thinner area of the total bank. Contrary to the front of the intertidal area (e.g. Figure 4) which represents the most thinner part of the intertidal zone, the front of the subtidal part is the more larger area of the mudbank. Therefore, the front of the mudbank constitute a bigger source of fluid mud during the migration processes.

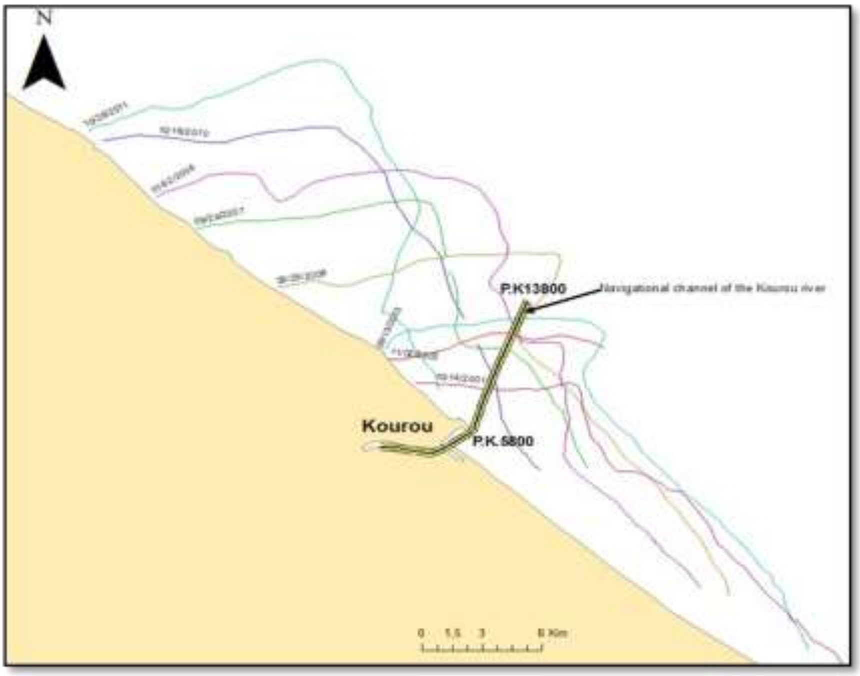

Figure 5. Localization of the subtidal area of the mudbank along the Kourou coast from 2001 to 2011, localization of the navigational channel of the Kourou river PK 5800 (at the mouth of the Kourou river) to PK 13800 (end of the channel)

3.2. What happens in the Kourou river?

Regular bathymetric surveys of the Kourou harbor channel offer a detailed situation of fluid mud arrival along the channel and so on the subtidal migration of the mudbank. Fresh mud arrival in the Kourou channel induces significant depth addition, more precisely the mud lens, furthermore important dredging effort in the navigation channel is organized to allow the passage of economical shipping. This mud lens represents a significant layer of fluid mud which overlay the consolidated bed. In fact, fluid mud is easily transported through the coastal current and could be deposited on other layer of consolidated mud. The bathymetric survey highlights the displacement of the bank along the navigation channel during the measurement period.

During the study period, sporadic events of important arrival of fresh mud in the Kourou harbor channel were observed (e.g. Figure 6). The lack of hydrodynamic data near this coastal site do not permit a coupling between the sporadic silting-up and eventual changes of the hydrodynamic conditions, and thus explanation of these arrival of fluid mud only could be coupling by the position of the mudbank. Heterogeneity of the mud thickness in the channel is denoted depending on the localization across the harbor channel, more precisely the distance from the coast.

Silting-up of the channel was first observed from the mid-2004, the dredging effort were then concentrated from the PK 8000 (approx. mid-channel) to offshore, in order to liberate the navigational channel. Generally between June 2002 and April 2010 (except in the beginning of 2008), thinner mud thickness were observed at the mouth of the Kourou river (near PK 5800).

Between June 2002 and July 2004, more important mud thickness were observed between PK 7800 and PK 9800 oscillated from 0.75m to 2m. The extremity of the navigational cannel encountered less arrival of fluid mud as indicated by the in-situ measurement. Between November 2007 to June 2008, important fresh arrival of mud were observed in the internal channel from PK 5800.

From 2001 to 2004, the curving subtidal part, and therefore the more important part of the bank, was localized in front of the Kourou channel, and relatively less mud was encountered in the channel(e.g. Figures 5&6). Between 2003 and 2006, the mudbank was crossing the Kourou river, the major part of the bank was beyond the channel, we noted a stagnation and a slowing down of the bank migration, as the Kourou river constitute a natural barrier. As a contrary, since 2006

when the major part of the bank were situated after the Kourou river channel, it appears more faster migration of the mudbank.
The beginning of the channel river (from PK 5800 to 6500) seemed to be silting-up since 2010 (e.g. Figure 6) while the trailing edge of the Kourou bank was localized at the vicinity of the cannel (e.g. Figure 5). In fact, more consistent mud were found in this part of the channel during this period (2010 to 2012).

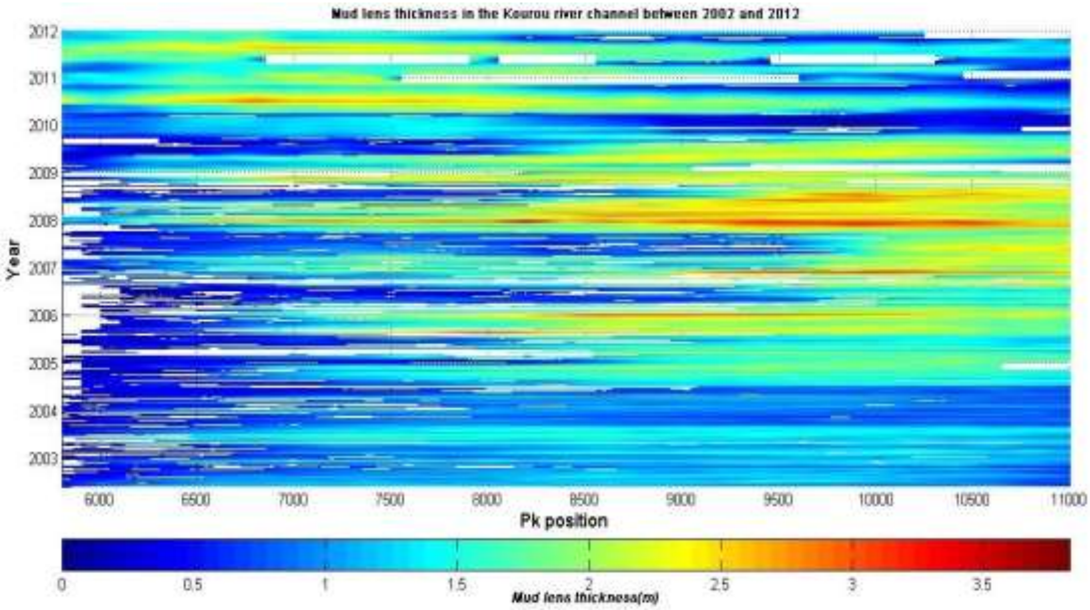

Figure 6. Mud lens thickness in the Kourou river channel between 2002 and 2012. PK 5800 indicate the position at the mouth of the Kourou river, the navigation channel end at the PK 14000 (not represented in this figure)

4. CONCLUSIONS

Mudbanks influence on the coast require intense monitoring in order to evaluate their spatial localization on the coast either during the bank or inter-bank phases. The study of the nearshore processes of mudbank had to be realize at different spatial and time-scale.
The first tools contribute to the localization of the bank with two and three-dimensional morphology characteristics such as an idea of the altitude of the mud, and the quantity of muddy sediment on the mudbank. While in-situ measurement is a support to remote sensing extracted data by consolidate the results obtained by satellite imagery by the quantification of the amount of mud present on the shore or estuary at the different stages of the mudbank migration.

ACKNOWLEDGEMENTS

The authors acknowledge various French research grants involving work on the Amazon-influenced coast of South America. These include funding by the Centre National d'Etudes Spatiales (CNES), by the Institut National des Sciences de l'Univers (INSU), and by the Université du Littoral Côte d'Opale (ULCO). Part of these results has been acquired in the Infolittoral Project. CP is supported by a PhD studentship from the Centre National d'Etudes Spatiales (CNES) and the Centre National de la Recherche Scientifique (CNRS).

REFERENCES

Anthony E.J., Gardel A., Gratiot N., Proisy C., Allison M.A., Dolique F.,Fromard F.,2010. The Amazon- influenced muddy coast of South America: A review of mud-bank-shoreline interactions. Earth Science Reviews, Volume 103, Issues 3-4, pp.99-121

Anthony E.J, and Dolique F., 2004. The influence of Amazon-derived mud banks on the morphology of sandy, headland-bound beaches in Cayenne, French Guiana: A short- to long-term perspective. Marine Geology, 208, pp.249-264.

Augustinus P.G.E.F., 1978. The changing

shoreline of Surinam (South America). PhD thesis, University of Utrecht, Utrecht, The Netherlands, pp.232.
Augustinus P.G.E.F., 2004. The influence of the trade winds on the coastal development of the Guianas at various scale levels: a synthesis. Marine Geology 208, pp.145-151.
Baghdadi N., Gratiot N., Lefebvre J.P., Oliveros C., and Bourguignon A., 2004. Coastline end mudbank monitoring in French Guiana: contributions of radar and optical satellite imagery. Canadian Journal of Remote Sensing, Vol.30, n°2, pp.109-122.
Froidefond J.M., Pujos M., and Andre X., 1988. Migration of mud-banks and changing coastline in French Guiana. Marine Geology, Vol.84, pp.19-30.
Gardel A., Gratiot N., 2004. Monitoring of coastal dynamics in French Guiana from 16years of SPOT Satellite Images. Journal of Coastal Research, SI 39, Proceedings of the 8th International Coastal Symposium), 1502-1505. Itajai, SC, Brazil, ISSN 0749-0208.
Gardel A., Gratiot N., 2005. A satellite image-based method for estimating rates of mud bank migration, French Guiana, South America, Journal of Coastal Research, Issue 21, pp.720-728.
Warne A.G, Meade R.H., White W.A., Guevara E.H., Gigeaut J., Smyth R.C., Aslan A. and Tremblay T., 2002. Regional controls on geomorphology, hydrology and ecosystem integrity in the Orinoco Delta, Venezuela. Geomophology, Vol. 44,pp. 273-307.

ECUADOR 1980 - 1983
CHILE 1983 - 1986
BRASIL 1986 - 1989
ARGENTINA 1989 - 1991
PERU 1991 - 1993
COLOMBIA 1993 - 1995
MEXICO 1995 - 1997
VENEZUELA 1997 - 1999
ARGENTINA 2000 - 2002
BOLIVIA 2002 - 2004
CHILE 2004 - 2006
COLOMBIA 2006 - 2008
CUBA 2008 - 2010
MEXICO 2010 - 2012
GUYANA FRANCESA 2012 - 2014